Curcumin-Loaded Polymeric Nanoparticles for Neuroprotection in Neonatal Rats with Hypoxic-Ischemic Encephalopathy (HIE)

Chih-Chung Chen

A thesis

submitted in partial fulfillment of the

requirements for the degree of

Master of Science

University of Washington

2017

Committee:

Elizabeth Nance

Shaoyi Jiang

Program Authorized to Offer Degree:

Chemical Engineering

University of Washington

Abstract

Curcumin-Loaded Polymeric Nanoparticles for Neuroprotection in Neonatal Rats with Hypoxic-Ischemic Encephalopathy (HIE)

Chih-Chung Chen

Chair of the Supervisory Committee:

Prof. Elizabeth Nance

Hypoxic-ischemic encephalopathy (HIE) is the leading cause of permanent brain injury and is due to a reduction in the supply of oxygen, compounded by low blood flow to the brain. Moderate to severe HIE is the major cause of morbidity and mortality in neonates around the time of birth. Current experimental evidence and clinical trials suggest that therapeutic hypothermia (TH) can reduce brain damage and improve neurological outcomes after neonatal hypoxic-ischemic (HI) injury. However, some infants still die and nearly half of affected infants continue to have significant brain injury in spite of treatment with TH. Therefore, additional treatment options should be explored. Curcumin has recently been found to have antioxidant, anti-inflammatory and anti-apoptotic effects that may mitigate the outcomes of brain injury after perinatal asphyxia. Nonetheless, curcumin has low solubility and limited ability to cross the blood-brain barrier (BBB). Several studies show that nanoparticles have the ability to cross the BBB, and incorporation of

curcumin into a nanoparticle platform can overcome therapeutic limitations for effective use. After crossing the BBB, nanoparticles must have the ability to travel through the brain parenchyma to reach diseased cells and deliver a therapeutic. Previously it has been found that poly(ethylene glycol) (PEG)-coated polystyrene particle less than 114 nm in diameter with a zeta (ζ)-potential more neutral than -6 mV can penetrate within the brain parenchyma. Using this criteria, the biodegradable polymer methoxy(polyethylene glycol)-poly(lactic-co-glycolic acid) (mPEG-PLGA) was used to prepare curcumin-loaded nanoparticles. The impact of nanoparticle formulation parameters on nanoparticle' size and ζ-potential was investigated. Curcumin loading and curcumin release kinetics from the nanoparticle were also studied. In addition, nanoparticle transport behavior in a rat brain *ex vivo* model was studied using a high resolution multiple particle tracking technique. The brain localization and biodistribution of the nanoparticle and preliminary efficacy study of the curcumin-loaded nanoparticle was studied in a postnatal day 7 (P7) HI rat model. It was found that the nanoprecipitation method is a feasible method to formulate both curcumin-loaded mPEG5k-PLGA45k (50:50) and PLGA45k (50:50) nanoparticles with 5 – 6% curcumin loading. mPEG5k-PLGA45k (50:50) surface-coated with 1% F127 had better mobility within the brain parenchyma than PLGA45k (50:50) and both nanoparticles had good stability and sustained curcumin release within 24 hours. Preliminary results also showed that mPEG5k-PLGA45k (50:50) was able to get into the brain and curcumin-loaded mPEG5k-PLGA45k (50:50) increased curcumin passage across the BBB and reduced neuronal injury in the HIE rat model.

Key words: curcumin, nanoparticle, drug delivery, HIE

Acknowledgements

First or all, I would like to thank my advisor, Dr. Elizabeth Nance, for her research and future path advice, and giving me the opportunity to work in her lab. I really appreciate her for mentoring my research project, thesis, and being a role model as a researcher and always being there to support me. I have enjoyed the lab environment and I have learned a lot from all the lab members in our lab. I also would like to thank Dr. Shaoyi Jiang for reading my thesis.

I would like to thank all the lab members in our lab for giving me many supports, especially Rick Liao, Chad Curtis, Mengying Zhang, Andrea Joseph, Michael McKenna, who are all the Ph.D. students in our lab, Sanchit Gad, Cayen Panlilio and Holly Sullivan, who are three of the undergraduates in our lab. I thank Rick Liao and Andrea Joseph for always giving me some suggestions, supporting and always being willing to discuss my research project with me leading me to try several ideas that I might not have tried otherwise. I thank Chad Curtis for helping me a lot on the python code and nanoparticle's diffusivity perspective. I thank Mengying Zhang, Michael Mckenna and Holly Sullivan for helping me a lot on the confocal imaging and brain section. I thank Sanchit Gad and Cayen Panlilio for always being there and covering me when I was busy. I thank Prof. Pratik Parikh for letting me have the opportunity to work on curcumin's efficacy and biodistribution study that inspired my interest in the research and is a tough and super exciting research. I also thank Dr. Tommy Wood and Kylie Corry for introducing me to the clinical and animal perspectives.

Lastly, I would like to express my gratitude to my lovely family and all my important friends in Taiwan or in other countries, and all my friends I met in Seattle. I really appreciate all their infinite and unconditional love and support and kindly sparing their time to talk with me when I felt sad.

Table of Contents

List of Tables

List of Figures

Chapter 1 Introduction and Background

Hypoxic-ischemic encephalopathy (HIE) is the leading cause of permanent brain injury due to a reduction in the supply of oxygen, compounded by low blood flow to the brain [1, 2]. Moderate to severe HIE after perinatal asphyxia is a major cause of morbidity and mortality in neonates around the time of birth [3, 4]. The extent of cerebral injury following HIE depends on the balance between the causative mechanisms of irreversible injury, such as neuronal necrosis or persistent inflammation, and endogenous protection (acute phase response, recovery, and neuronal repair) [5]. Unfortunately, perinatal asphyxia is difficult to prevent or predict, and despite important progress in neonatal and obstetrical care, rates of perinatal asphyxia in term newborns have remained unchanged at around 2-4 per 1000 live births [1, 6]. Of affected newborns, 15%-20% of affected newborns will die in the postnatal period, and an additional 25% will develop severe and permanent neuropsychological sequelae, including mental retardation, visual motor or visual perceptive dysfunction, increased hyperactivity, cerebral palsy, and epilepsy [1]. The outcomes of HIE are devastating and permanent, making it a major burden for the patient, the family, and society [1]. Therefore, researchers and clinicians are still having a great predicaments on treating newborn infants with HIE and having to start treatment for them right after the primary neurological injury has started, where we are still unknown how the severity of the injury will go.

More than a decade ago, experimental evidence and clinical trials suggested that therapeutic hypothermia (TH) reduces brain damage and improves neurological outcome after neonatal hypoxic-ischemic (HI) injury [5]. The neuroprotective strategy of TH involves the modulation of some irreversible injury mechanisms, providing an endogenous neuroprotective effect and

resulting in a reduction of cerebral metabolism by approximately 5% for each 1°C decrease in body temperature, which delays the onset of anoxic cell depolarization [5]. TH inhibits an inflammatory cascade, reduces production of reactive oxygen species, and reduces metabolic rate with reduced oxygen consumption and carbon dioxide production [5, 7-10]. There is evidence demonstrating that induced hypothermia (33.5-34.5°C), when started within the 6 hour window after the birth of full-term asphyxiated newborns, is beneficial in reducing mortality and neurodevelopmental delay assessed by the Bayley scale in the follow-up at 18 months of life [11-15]. There are two TH methods, including selective head hypothermia and total body hypothermia. Selective head hypothermia [11] reduces temperature to 34.5°C, and total body hypothermia reduces temperature to 33.5°C [13]. Both techniques recommend maintenance at these respective temperatures for 72 hours. After hypothermia, the rewarming phase must be slow and gradual, and conducted over a 4-hour time period, with temperature increase at a speed of 0.5°C per hour until the temperature reaches 36.5°C [5]. This process aims to prevent complications caused by rapid rewarming [3, 16]. The temperature must remain above 33°C during the entire hypothermia period. Temperatures lower than 32°C are less neuroprotective, and very severe systemic adverse effects and increased mortality have been observed with temperatures below 30°C [3, 16]. However, some infants still die or survive with sequelae at varying levels, and nearly half of affected infants continue to have significant brain injury despite treatment with TH. [17]. The best result in terms of TH seems to be in mild to moderate injuries, while the real benefit has been questioned for infants with severe encephalopathy [5]. Furthermore, TH only offers a 15% risk reduction in death and disability and may harm infants born with certain co-morbidities such as infections or bleeding [18, 19]. Other neuroprotective agents like Erythropoietin (Epo) [20], N-acetyl cysteine (NAC) [21] and xenon [22] are considered as an adjuvant to TH, but high doses are usually needed and may cause some

side effects, like hypertension, clotting, seizures and death, and they are often combined with TH [23]. Thus, the need for the strategies that can provide better neuroprotection than TH are necessary.

Curcumin is an attractive therapy for neuroprotection and treatment of brain injuries. It has recently been found to have antioxidant, anti-inflammatory, and anti-apoptotic effects [24, 25] that may mitigate the sequelae of oxygen and blood flow deprivation to the brain following perinatal asphyxia, and has been shown to induce neurogenesis [26]. It also prevents reduced docosahexaenoic acid (DHA) content, whose deficiency is linked to several neurocognitive disorders in the brain following brain trauma. [25]. Curcumin also promotes neurite outgrowth and proliferation of neuronal stem cells (NSC) *in vitro* and *in vivo* (through activation of the ERK and MAP kinase pathways) [27, 28]. In addition, it plays a role in neurogenesis, synaptogenesis, and migration of neural progenitor cells (NPCs) *in vitro* [29]. Its role in neurogenesis would be an important neuroprotective and reparative mechanism in neonatal HIE. These effects have led to improvement in brain health by reducing degeneration after HI injury, oxidative damage, and traumatic brain injury [30]. However, curcumin has low aqueous solubility and poor bioavailability due to its hydrophobic nature, and has not yet been approved as a therapeutic agent in spite of its *in vitro* and *in vivo* efficacy and its safety [31, 32]. Its rapid hepatic metabolism also decreases its efficacy, requiring higher doses to compensate, which might cause some side effects. Thus, to improve curcumin's bioavailability, stability and therapeutic applications, incorporation of curcumin into a nanoparticle platform will alleviate the current curcumin's therapeutic limitations for effective use.

In order to successfully get into the brain and provide therapeutic effects on the targeted cells affected by the HI injury, the therapeutic needs to first cross the blood-brain barrier (BBB) [33], which is formed by brain endothelial cells (ECs) and is a highly selective semipermeable membrane that prevents most compounds from penetrating into the brain. Tight junctions and adheren junctions between the ECs further block the free diffusion of polar solutes from blood to brain interstitial fluid. Only those that are small and lipophilic or those that enter the brain through an active transport mechanism, particularly with essential nutrients, precursors and cofactors, are allowed to cross the BBB. Once across the BBB, they must have the ability to move within the brain parenchyma, which in itself contains multiple barriers, such as the geometry of the pores that exist between the cells, any obstruction present in the extracellular matrix (ECM), and binding functional groups extending from the surface of the cells (some of which may contain charge) [33]. Finally, the drug should get into specific cells. These are the reasons why it usually takes 35% longer to develop drugs for neurological disorders than those for other diseases in human beings [34]. The first successful delivery of a drug across the BBB occurred in 1995. It was a huge breakthrough in the nanoparticle drug delivery field, helping advance research and development toward clinical trials of nanoparticle delivery systems. Thus, nanoparticles can overcome all three of these barriers, if they are appropriately engineered based on the disease.

Nanotechnology provides a promising drug delivery platform for treatment of central nervous system (CNS) diseases. Nanoparticles typically have a diameter between 1 nm to 100 nm [35, 36], and can consist of a variety of materials, including polymer conjugates, polymeric nanoparticles, lipid-based nanoparticles, dendrimers, carbon nanotubes and gold nanoparticles [37]. Nanoparticles provide several advantages as drug carriers, such as high drug payload, protecting

drug from clearance by the immune system or rapid degradation, tunable drug release kinetics and functionalization with multiple targeting functional groups or ligands to increase nanoparticle's affinity for specific and targeted cells [37]. Nanoparticles also can increase drugs' solubility and reduce toxicity and side effects of drugs while maintaining their therapeutic effects [33]. Most important, nanoparticles have greater safety and biocompatibility.

Poly(lactic-co-glycolic acid) (PLGA), with a long history of safe use in humans, should facilitate translation and testing of therapeutic strategies in human clinical trials [38]. It is also a successful biodegradable polymer because it undergoes hydrolysis in the human body to produce the original monomers, lactic acid and glycolic acid [39]. These two monomers are by-products of various metabolic pathways in the body under normal physiological conditions. Most importantly, PLGA is FDA-approved. PLGA copolymer and its variants are commonly used in many pre-clinical studies to form nanoparticles that deliver therapeutics to treat several diseases.

However, PLGA is not able to diffuse a long distance to reach the diseased cells in the brain [38]. Hence, a polyethylene glycol (PEG) layer is important for nanoparticles used as drug delivery systems. PEG is a safe, hydrophilic, and uncharged polymer. It sterically stabilizes nanoparticle suspensions, minimizes non-specific protein absorption, reduces interactions within biological medium [38], and decreases recognition by the mononuclear phagocyte system (MPS) [40]. In 2012, Nance and coworkers [38] analyzed the diffusion rates of densely PEG-coated versus standard COOH-coated nanoparticles of various sizes in human and rat brain tissues as well as in the living mouse brain. They found that with a dense PEG coating, which minimizes adhesive interactions, nanoparticles up to 114 nm and with near-neutral ZP can diffuse within the human

brain tissue. These nanoparticles can achieve a long circulation time, high drug payload, and sustained therapeutic release. For those without densely PEG-coated nanoparticles, even the 40-nm nanoparticles were immobile. Nanoparticle surface properties also influence nanoparticle behavior. In 2011, Kulkarni and coworkers [41] investigated different surface modifications' on delivery efficiency of nanoparticles across the BBB. They found that distribution of the nanoparticles within the liver, spleen, lungs and brain is significantly altered after surface coating with poloxamer 188 (F68), pluronic F-127 (F127) and polysorbate 80 (P80). Most importantly, these surfactants did increase nanoparticle uptake in the brain. Taken together, these findings demonstrate PLGA with a dense PEG coating and appropriate surface modification is a feasible and efficient strategy to deliver therapeutic agents across the BBB.

Due to the important issues from HIE with no effective treatment up to now, and due to curcumin's pleiotrophic effects and nanoparticle's potential advantages as introduced previously, my research is focused on formulating curcumin-loaded polymeric nanoparticles to overcome TH's current predicaments on treating HIE, with the goal to provide better neuroprotection to the brain with HI injury. There are four chapters in my research. Chapter 1 is an introduction and background. Chapter 2 will focus on formulation and optimization of curcumin-loaded polymeric nanoparticles. Chapter 3 will focus on the effective diffusivity and biodistribution of nanoparticles in neonatal rat brain. Chapter 4 will focus on preliminary efficacy study of curcumin-loaded mPEG5k-PLGA45k (50:50) nanoparticles in the neonatal HIE rat model.

Chapter 2 Formulation and Optimization of Curcumin-loaded Polymeric Nanoparticles

2.1 Materials and Methods

2.1.1 Particle Preparation

The nanoparticles were prepared by one of two methods: the single emulsion method or the nanoprecipitation method. The nanoparticles were all collected by normal centrifugation and then washed twice by 1 mL deionized water (DI) water or 1x phosphate-buffered saline (PBS; Corning, Corning, NY). Size, polydispersity index (PDI) and ζ-potential of the nanoparticles were determined using dynamic light scattering (DLS, Malvern).

2.1.1.1 The Nanoprecipitation Method

mPEG5k–PLGA45k (50:50) (Akina, Inc., West Lafayette, IN) or PLGA45k (50:50) (Sigma-Aldrich, St Louis, MO) polymers were dissolved in acetone (ACN; Fisher Chemical, Pittsburgh, PA) with 10% target curcumin loading, unless specified otherwise. The polymer solution (organic phase) was then added dropwise into 25 mL surfactant solutions where nanoparticles were formed spontaneously and were stirred for 3 h to remove the organic solvent. The organic solvent was further removed by using rotary evaporator under reduced pressure, 15 mbar, at 4ºC for 20 minutes. Nanoparticles were collected and washed twice by normal centrifugation with DI water. Finally, the nanoparticles were resuspended in 1 mL DI water, or in 1x PBS if the nanoparticles were prepared to be used in the animal experiments. Nanoparticles were used immediately or had 20% (w/v) sucrose added as a cryoprotectant and lyophilized and stored at -80ºC until further use.

2.1.1.2 The Single Emulsion Method

mPEG5k-PLGA45k (50:50) or PLGA45k(50:50) polymers were dissolved in organic solvents with 10% target drug loading, unless specified otherwise. The solution was then added into 5 mL 0.5% surfactant solutions immediately followed by sonication using a microtip probe sonicator (Fisher Scientific, Pittsburgh, PA) in a water-ice bath for 1 minute at 30% amplitude (1 second on/1 second off). The emulsified solution was immediately poured into 25 mL 1% surfactant solutions, and was stirred magnetically at speed 700 rpm for 3 h. The organic solvent was further removed by using rotary evaporator under reduced pressure, 15 mbar, at 4ºC for 30 minutes. Nanoparticles were collected and washed twice by normal centrifugation with DI water. Finally, the nanoparticles were resuspended in 1 mL DI water or 1x PBS if the nanoparticles were prepared to be used in the animal experiments. Nanoparticles were used immediately, or had 20% (w/v) sucrose added as a cryoprotectant and lyophilized and stored at -80ºC until further use.

2.1.2 Nanoparticle Characterization

The size (hydrodynamic diameter), polydispersity index (PDI) and zeta potential (ζ-potential) measurements of the nanoparticles were obtained by using a Zetasizer Nano instrument (Malvern Instruments, Malvern, UK). Size and PDI were determined by DLS, performed at 25ºC at a scattering angle of 173◦. ζ-potential was determined by laser Doppler anemometry. Samples were diluted to appropriate concentrations to obtain accurate measurements in 10 mM sodium chloride (NaCl), pH 7.4. as described previously [42].

2.1.3 Drug Loading and Drug Encapsulation Efficiency

Curcumin-loaded mPEG5k-PLGA45k (50:50) or PLGA45k (50:50) nanoparticles were prepared and collected as described in the **Section 2.1.1.1** and **2.1.1.2**. The drug loading and drug encapsulation efficiency of the curcumin-loaded nanoparticles was measured by dissolving the lyophilized nanoparticles in dimethyl sulfoxide (DMSO; Macron Fine Chemicals, Center Valley, PA) and measuring the absorbance at 430 nm using an ultraviolet-visible spectroscopy (UV-vis; SpectraMax M5, Molecular Devices, Sunnyvale, CA). The curcumin content was determined by comparing to a calibration curve (concentration range of 0-100 μg/mL). Absorbance of the blank nanoparticles in DMSO at the same polymer concentration was subtracted [43]. Drug loading (DL) and drug encapsulation efficiency (DEE) were calculated as follows:

$$\text{Drug loading (\%)} = \frac{weight\ of\ drug\ entrapped\ within\ nanoparticles}{total\ weight\ of\ nanoparticles} \times 100\%$$

$$\text{Drug encapsulation efficiency (\%)} = \frac{weight\ of\ drug\ entrapped\ within\ nanoparticles}{total\ drug\ added} \times 100\%$$

2.1.4 Nanoparticle Morphology

The morphology of the curcumin-loaded polymeric nanoparticles (PLGA, mPEG-PLGA) and blank mPEG5k-PLGA45k (50:50) and PLGA45k (50:50) nanoparticles was measured by the XL830 scanning electron microscope (SEM) in the University of Washington Molecular Analysis Facility. SEM samples were prepared as follows: fresh curcumin-loaded nanoparticles were mixed with ethanol (Decon Laboratories, Inc., King of Prussia, PA) to dilute SEM sample's concentration. The solution was then dropped on a silicon wafer and the silicon wafer was put in a vacuum

desiccator at room temperature to dry the sample. After the evaporation, the sample was sputter coated with a 13 nm layer of Au/Pd and imaged.

2.1.5 *In Vitro* Curcumin Release

Curcumin-loaded mPEG5k-PLGA45k (50:50) and PLGA45k (50:50) nanoparticles were resuspended in 1 mL 50% (v/v) ethanol. Each sample was evenly distributed to three dialysis tubing cellulose ester membranes (MWCO: 300kDa, Spectrum Laboratories, Inc.) (N=3). The membranes were submerged in 20 mL 50% (v/v) ethanol and were placed on a shaker at 60 rpm at 37ºC. At designated time points, the membranes were transferred to fresh 20 mL 50% (v/v) ethanol. From the supernatants collected at each time point, curcumin content was determined by high-performance liquid chromatograph (HPLC) and UV-vis spectroscopy. Percent curcumin released from the nanoparticles was defined as the curcumin amount released at a specific time point divided by the total curcumin encapsulated in the nanoparticles.

2.1.5.1 UV-vis Spectroscopy Measurement

The *in vitro* curcumin release was measured by dissolving the lyophilized nanoparticles in DMSO and measuring the absorbance at 430 nm using ultraviolet-visible spectroscopy (SpectraMax M5, Molecular Devices, Sunnyvale, CA). The curcumin content was determined by comparing to a calibration curve (concentration range of 0-100 μg/mL). Absorbance of blank nanoparticles in DMSO at the same polymer concentration was subtracted [43].

2.1.5.2 High-Performance Liquid Chromatography (HPLC) Measurement

The supernatants collected at each time point were injected into a Shimadzu HPLC equipped with a C18 reverse phase column (5 μm, 4.6×150 mm; Agilent, Santa Clara, CA). Curcumin was eluted using two mobile phases, 0.1% (v/v) formic acid (Sigma-Aldrich, St Louis, MO) in HPLC grade H_2O (Honeywell, Morris Plains, NJ) and 0.1% (v/v) formic acid in HPLC grade acetonitrile (Fluka, Milwaukee, WI), at 0.8 mL/min and detected at 262 nm wavelength by an UV detector. The data were analyzed using LC solution software (Shimadzu Scientific Instruments) to acquire the curcumin concentration of the supernatants in each time point.

2.1.6 Statistical Analysis

Statistical analysis was performed by using a student t test. A p value < 0.05 was considered statistically significant.

2.2 Results

2.2.1 Nanoparticles Formulated by the Single Emulsion Method

2.2.1.1 Effect of PEG on Nanoparticle Characteristics

Curcumin-loaded mPEG5k-PLGA45k (50:50) and curcumin-loaded PLGA45k (50:50) nanoparticles were formulated with dichloromethane (DCM; Fisher Chemical, Pittsburgh, PA) as the organic solvent and 1% (w/v) polyvinyl alcohol (PVA; Sigma-Aldrich, St Louis, MO) as the surfactant with 27 mg/mL polymer concentration. Nanoparticles were collected by normal

centrifugation and washed twice in DI water. The size, PDI and ζ-potential of the nanoparticles are shown in **Table 2-1**. mPEG5k-PLGA45k (50:50) nanoparticles generally had a smaller size ($p < 0.05$) than PLGA45k (50:50) nanoparticles. Presumably, the PEG layer would help shield the PLGA core from the outside aqueous phase, stabilize and prevent nanoparticles from aggregating together.

2.2.1.2 Effect of Polymer Concentration on Nanoparticle Characteristics

2.2.1.2.1 Effect of Polymer Concentration on mPEG5k-PLGA45k (50:50) Nanoparticle Characteristics

Curcumin-loaded mPEG5k-PLGA45k (50:50) nanoparticles were formulated with DCM and 1% (w/v) PVA surfactant with 20, 27 or 50 mg/mL polymer concentration. Nanoparticles were collected by normal centrifugation and washed twice in DI water. The size, PDI and ζ-potential of the nanoparticles are shown in **Table 2-2**. Higher polymer concentration led to an increase in nanoparticle size from 27 mg/mL to 50 mg/mL ($p < 0.05$), but no significant difference from 20 mg/mL to 27 mg/mL ($p > 0.05$). The ζ-potential remained almost neutral and there was no difference when the polymer concentration increased.

2.2.1.2.2 Effect of Polymer Concentration on PLGA45k (50:50) Nanoparticle Characteristics

Curcumin-loaded PLGA45k (50:50) nanoparticles were formulated with DCM and 1% (w/v) PVA surfactant with 10 or 27 mg/mL polymer concentration. Nanoparticles were collected by normal centrifugation and washed twice in DI water. The size, PDI and ζ-potential of the nanoparticles

are shown in **Table 2-3**. The size of the nanoparticle slightly increased ~15 nm when the polymer concentration increased from 10 mg/mL to 27 mg/mL, but without significance ($p > 0.05$). No significant difference in ζ-potential was seen when the polymer concentration was increased ($p > 0.05$).

2.2.1.3 Effect of Organic Solvent on Nanoparticle Characteristics

2.2.1.3.1 Effect of EtAc and DCM on mPEG5k-PLGA45k (50:50) Nanoparticle Characteristics

Curcumin-loaded mPEG5k-PLGA45k (50:50) nanoparticles were formulated in DCM or ethyl acetate (EtAc; Macron Fine Chemicals, Center Valley, PA) and 1% (w/v) PVA surfactant with 20 mg/mL polymer concentration. Nanoparticles were collected by normal centrifugation and washed twice in DI water. The size, PDI and ζ-potential of the nanoparticles are shown in **Table 2-4**. EtAc generally produced a smaller size nanoparticle than those made in DCM ($p < 0.05$). No difference was seen in PDI ($p > 0.05$).

2.2.1.3.2 Effect of EtAc and DCM on PLGA45k (50:50) Nanoparticle Characteristics

Curcumin-loaded PLGA45k (50:50) nanoparticles were formulated in DCM or EtAc and 1% (w/v) PVA surfactant with 10 mg/mL polymer concentration. Nanoparticles were collected by normal centrifugation and washed twice in DI water. The size, PDI and ζ-potential of the nanoparticles are shown in **Table 2-5**. EtAc produced a nanoparticle that was 50 nm smaller in size compared to nanoparticles made in DCM.

2.2.1.4 Effect of Surfactant on Nanoparticle Characteristics

2.2.1.4.1 Effect of 1% PVA and 1% CHA on mPEG5k-PLGA45k (50:50) Nanoparticle Characteristics

Curcumin-loaded mPEG5k-PLGA45k (50:50) nanoparticles were formulated in DCM and 1% (w/v) PVA or 1% (w/v) CHA surfactant with 20 mg/mL polymer concentration. Nanoparticles were collected by normal centrifugation and washed twice in DI water. The size, PDI and ζ-potential of the nanoparticles are shown in **Table 2-6**. 1% (w/v) CHA led to a smaller (50 nm decrease in the size) and more uniform size nanoparticle but with a slightly more negative ζ-potential ($p < 0.05$ for both cases).

2.2.1.4.2 Effect of 1% PVA and 1% CHA on PLGA45k (50:50) Nanoparticle Characteristics

Curcumin-loaded PLGA45k (50:50) nanoparticles were formulated in DCM and 1% (w/v) PVA or 1% (w/v) CHA surfactant with 27 mg/mL polymer concentration. Nanoparticles were collected by normal centrifugation and washed twice in DI water. The size, PDI and ζ-potential of the nanoparticles are shown in **Table 2-7**. 1% (w/v) CHA and 1% (w/v) PVA resulted in a similar effect on PLGA45k (50:50) nanoparticles. The size of the nanoparticle significantly decreased by around 150 nm when change the surfactant from 1% (w/v) PVA to 1% (w/v) CHA.

2.2.1.5 Effect of Organic Solvent and Surfactant on Curcumin Loading

2.2.1.5.1 Effect of EtAc and DCM on Curcumin Loading

Curcumin-loaded mPEG5k-PLGA45k (50:50) nanoparticles were formulated in DCM or EtAc and 1% (w/v) PVA surfactant with 20 mg/mL polymer concentration. Nanoparticles were collected by normal centrifugation and washed twice in DI water. The curcumin loading and curcumin encapsulation efficiency of the nanoparticles are shown in Table 2-8. EtAc and DCM had no significant effect on the curcumin loading of the nanoparticle ($p > 0.05$).

2.2.1.5.2 Effect of 1% PVA and 1% CHA on Curcumin Loading

Curcumin-loaded mPEG5k-PLGA45k (50:50) nanoparticles were formulated in DCM and 1% (w/v) PVA or 1% (w/v) CHA surfactant with 20 mg/mL polymer concentration. Nanoparticles were collected by normal centrifugation and washed twice in DI water. The curcumin loading and curcumin encapsulation efficiency of the nanoparticles are shown in **Table 2-9**. The curcumin loading greatly decreased from around 6.35% to around 0.06% when the surfactant was changed from 1% (w/v) PVA to 1% (w/v) CHA ($p < 0.05$).

2.2.1.6 The stability of curcumin-loaded polymeric nanoparticles

Curcumin-loaded polymeric nanoparticles made from the single emulsion method were not stable as some chunks could be seen after resuspension, as shown in **Table 2-15** The stability of curcumin-loaded polymeric nanoparticles after 24 h.

Polymer	Polymer Concentration (mg/mL)	Organic Solvent	Surfactant	Mean Hydrodynamic Size ± SEM (nm)	PDI ± SEM	ζ-potential ± SEM (mV)
mPEG5k-PLGA45k (50:50)	20	ACN	1% F127	58.385 ± 2.289	0.063 ± 0.018	-3.748 ± 1.487
After 1 day	20	ACN	1% F127	57.447 ± 1.862	0.112 ± 0.052	-3.597 ± 1.193

Data are presented as average of N=2 batches.

SEM: standard error

Figure 2-1. The nanoprecipitation method therefore was another formulation method we used to formulate curcumin-loaded polymeric nanoparticles.

2.2.2 Nanoparticles formulated by the nanoprecipitation method

2.2.2.1 Nanoparticles formulated by the nanoprecipitation method

Curcumin-loaded mPEG5k-PLGA45k (50:50) nanoparticles were formulated in ACN and 1% (w/v) Pluronic® F-127 (F127; Sigma-Aldrich, St Louis, MO) surfactant with 20 mg/mL polymer concentration. Curcumin-loaded PLGA45k (50:50) nanoparticles were formulated in acetone and 1% (w/v) F127 surfactant with 5 mg/mL polymer concentration. Nanoparticles were all collected by normal centrifugation and washed twice in DI water. The size, PDI and ζ-potential of the nanoparticles are shown in **Table 2-10**. Particles made via nanoprecipitation with 1% (w/v) F127 and ACN is a feasible way to formulate similar and comparable results on the size, PDI, and ζ-potential of mPEG5k-PLGA45k (50:50) and PLGA45k (50:50) nanoparticles.

2.2.2.2 Effect of Polymer Concentration on Nanoparticle Characteristics

2.2.2.2.1 Effect of Polymer Concentration on mPEG5k-PLGA45k (50:50) Nanoparticle Characteristics

Curcumin-loaded mPEG5k-PLGA45k (50:50) nanoparticles were formulated in ACN and 1% (w/v) F127 surfactant with 20 or 50 mg/mL polymer concentration. Nanoparticles were collected by normal centrifugation and washed twice in DI water. The size, PDI and ζ-potential of the

nanoparticles are shown in **Table 2-11**. The size of the nanoparticles greatly increased from 60 nm to 97 nm when the polymer concentration increased from 20 mg/mL to 50 mg/mL ($p < 0.05$).

2.2.2.2.2 Effect of Polymer Concentration on PLGA45k (50:50) Nanoparticle Characteristics

Curcumin-loaded PLGA45k (50:50) nanoparticles were formulated in ACN and 1% (w/v) F127 surfactant with 5 or 20 mg/mL polymer concentration. Nanoparticles were collected by normal centrifugation and washed twice in DI water. The size, PDI and ζ-potential of the nanoparticles are shown in **Table 2-12**. Change in polymer concentration led to a similar effect on the PLGA45k (50:50) nanoparticles as it did on the mPEG5k-PLGA45k nanoparticles. The size of the nanoparticle increased from 60 nm to 145 nm when the polymer concentration increased from 5 mg/mL to 20 mg/mL.

2.2.2.3 Effect of the Amount of Polymer Used in Formulation on Nanoparticle Characteristics

Curcumin-loaded mPEG5k-PLGA45k (50:50) nanoparticles were formulated in ACN and 1% (w/v) F127 surfactant with 50 mg/mL polymer concentration using 50 mg curcumin dissolved in 1 mL ACN or 10 mg curcumin dissolved in 0.2 mL ACN. Nanoparticles were collected by normal centrifugation and washed twice in DI water. The size, PDI and ζ-potential of the nanoparticles are shown in **Table 2-13**. The polymer amount used in formulation did not influence the size when the polymer concentration was kept unchanged, but did influence the nanoparticles PDI.

2.2.2.4 Curcumin Loading

Curcumin-loaded mPEG5k-PLGA45k (50:50) nanoparticles were formulated in ACN and 1% (w/v) F127 surfactant with 20 mg/mL polymer concentration. Curcumin-loaded PLGA45k (50:50) nanoparticles were formulated in a similar condition, but with 5 mg/mL polymer concentration. Nanoparticles were collected by normal centrifugation and washed twice in DI water. The curcumin loading and curcumin encapsulation efficiency of the nanoparticles are shown in **Table 2-14**. Particles made using nanoprecipitation with 1% (w/v) F127 and ACN represented a feasible way to formulate similar and comparable results on the size, PDI, ζ-potential and curcumin loading of mPEG5k-PLGA45k (50:50) and PLGA45k (50:50) nanoparticles.

2.2.2.5 The Stability of the Curcumin-loaded Polymeric Nanoparticle

The stability of the curcumin-loaded mPEG5k-PLGA45k (50:50) nanoparticle was measured by DLS and Zetasizer. The size, PDI and ζ-potential of the nanoparticle remained unchanged after 24 h and the results are shown in **Table 2-15**. Moreover, no chunks were seen after 24 h, as shown in **Figure 2-2**.

2.2.2.6 SEM Characterization of Nanoparticle Morphology

The morphology of curcumin-loaded mPEG5k-PLGA45k (50:50) and PLGA45k (50:50) nanoparticles and empty mPEG5k-PLGA45k (50:50) and PLGA45k (50:50) nanoparticles is shown in **Figure 2-3**. These nanoparticles were all spherical in shape, consistent with the size results from DLS.

2.2.2.7 *In Vitro* Curcumin Release Kinetics from mPEG5k-PLGA45k (50:50) and PLGA45k (50:50) Nanoparticles

Based on the data above, the curcumin-loaded polymeric nanoparticles made from the nanoprecipitation method with 1% (w/v) F127 and ACN had good stability and comparable results on the size, PDI, ζ-potential and curcumin loading between mPEG5k-PLGA45k (50:50) and PLGA45k (50:50) nanoparticles. The release kinetics of these curcumin-loaded polymeric nanoparticles was also investigated by HPLC as shown in **Figure 2-3** Assessment of curcumin-loaded polymeric nanoparticle morphology using SEM.

(A) Curcumin-loaded mPEG5k-PLGA45k (50:50)

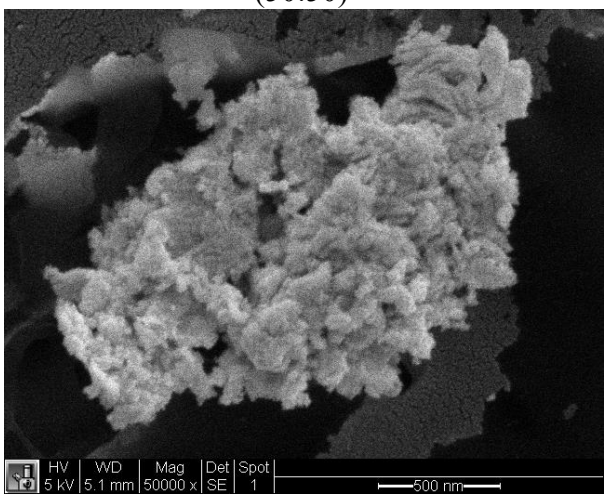

(B) Curcumin-loaded PLGA45k (50:50)

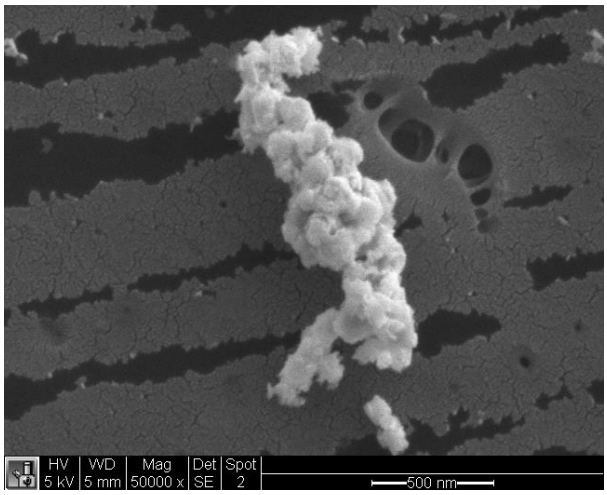

(C) Empty mPEG5k-PLGA45k (50:50)

(D) Empty PLGA45k (50:50)

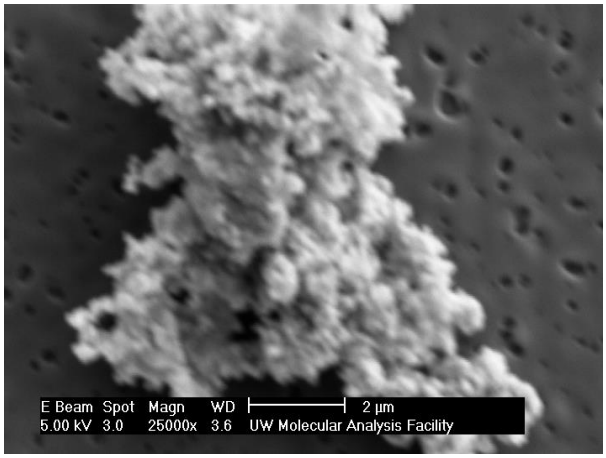
E Beam Spot Magn WD 2 µm
5.00 kV 3.0 25000x 3.6 UW Molecular Analysis Facility

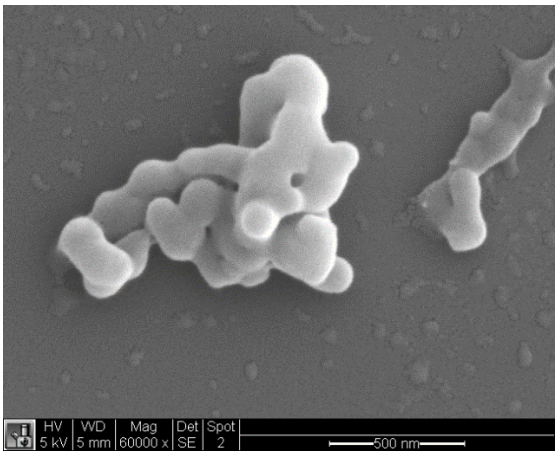
HV WD Mag Det Spot
5 kV 5 mm 60000 x SE 2
500 nm

Figure 2-4. Both mPEG5k-PLGA45k (50:50) and PLGA45k (50:50) nanoparticles could provide a sustained curcumin release over a 24 to 48 h time period. Nearly 100% curcumin was released from the mPEG5k-PLGA45k (50:50) nanoparticles, while only around 60% to 65% curcumin was released from the PLGA45k (50:50) nanoparticles.

Table 2-1 Effect of PEG on nanoparticle characteristics

Polymer	Polymer Concentration (mg/mL)	Organic Solvent	Surfactant	Mean Hydrodynamic Size ± SEM (nm)	PDI ± SEM	ζ-potential ± SEM (mV)
mPEG5k-PLGA45k (50:50)[a]	27	DCM	1% PVA	191.758 ± 28.246	0.230 ± 0.062	-1.527 ± 0.311
PLGA45k (50:50)[b]	27	DCM	1% PVA	287.767 ± 46.020	0.315 ± 0.067	-0.274 ± 0.054

[a] Data are presented as average of N=13 batches.
[b] Data are presented as average of N=3 batches.

SEM: standard error; PDI: polydispersity index

Table 2-2 Effect of polymer concentration on mPEG5k-PLGA45k (50:50) nanoparticle characteristics

Polymer	Polymer Concentration (mg/mL)	Organic Solvent	Surfactant	Mean Hydrodynamic Size ± SEM (nm)	PDI ± SEM	ζ-potential ± SEM (mV)
mPEG5k-PLGA45k (50:50)[a]	50	DCM	1% PVA	323.067 ± 46.724	0.152 ± 0.056	-1.755 ± 0.500
mPEG5k-PLGA45k (50:50)[b]	27	DCM	1% PVA	191.758 ± 28.246	0.230 ± 0.062	-1.527 ± 0.311
mPEG5k-PLGA45k (50:50)[c]	20	DCM	1% PVA	180.658 ± 13.701	0.238 ± 0.024	-1.115± 0.030

[a] Data are presented as average of N=5 batches.
[b] Data are presented as average of N=13 batches.
[c] Data are presented as average of N=4 batches.

SEM: standard error; PDI: polydispersity index

Table 2-3 Effect of polymer concentration on PLGA45k (50:50) nanoparticle characteristics

Polymer	Polymer Concentration (mg/mL)	Organic Solvent	Surfactant	Mean Hydrodynamic Size ± SEM (nm)	PDI ± SEM	ζ-potential ± SEM (mV)
PLGA45k (50:50)[a]	27	DCM	1% PVA	287.767 ± 46.020	0.315 ± 0.067	-0.274 ± 0.054
PLGA45k (50:50)[b]	10	DCM	1% PVA	272.933 ± 36.204	0.303 ± 0.219	-2.852 ± 3.683

[a] Data are presented as average of N=3 batches.
[b] Data are presented as average of N=3 batches.

SEM: standard error; PDI: polydispersity index

Table 2-4 Effect of EtAc and DCM on mPEG5k-PLGA45k (50:50) nanoparticle characteristics

Polymer	Polymer Concentration (mg/mL)	Organic Solvent	Surfactant	Mean Hydrodynamic Size ± SEM (nm)	PDI ± SEM	ζ-potential ± SEM (mV)
mPEG5k-PLGA45k (50:50)[a]	20	EtAc	1% PVA	152.753 ± 16.749	0.238 ± 0.076	-2.206 ± 0.523
mPEG5k-PLGA45k (50:50)[b]	20	DCM	1% PVA	176.305 ± 14.258	0.227 ± 0.024	-1.108 ± 0.402

[a] Data are presented as average of N=13 batches.
[b] Data are presented as average of N=7 batches.

SEM: standard error; PDI: polydispersity index

Table 2-5 Effect of EtAc and DCM on PLGA45k (50:50) nanoparticle characteristics

Polymer	Polymer Concentration (mg/mL)	Organic Solvent	Surfactant	Mean Hydrodynamic Size ± SEM (nm)	PDI ± SEM	ζ-potential ± SEM (mV)
PLGA45k (50:50)[a]	10	EtAc	1% PVA	247.333 ± 43.260	0.457 ± 0.142	-5.457 ± 0.444
PLGA45k (50:50)[b]	10	DCM	1% PVA	300.833 ± 3.253	0.431 ± 0.400	-0.265 ± 0.025

[a] Data are presented as average of N=2 batches.
[b] Data are presented as average of N=2 batches.

SEM: standard error; PDI: polydispersity index

Table 2-6 Effect of 1% PVA and 1% CHA on mPEG5k-PLGA45k (50:50) nanoparticle characteristics

Polymer	Polymer Concentration (mg/mL)	Organic Solvent	Surfactant	Mean Hydrodynamic Size ± SEM (nm)	PDI ± SEM	ζ-potential ± SEM (mV)
mPEG5k-PLGA45k (50:50)[a]	20	DCM	1% CHA	125.998 ± 18.992	0.113 ± 0.0634	-5.088 ± 2.388
mPEG5k-PLGA45k (50:50)[b]	20	DCM	1% PVA	176.305 ± 14.258	0.227 ± 0.024	-1.108 ± 0.402

[a] Data are presented as average of N=4 batches.
[b] Data are presented as average of N=7 batches.

SEM: standard error; PDI: polydispersity index

Table 2-7 Effect of 1% PVA and 1% CHA on PLGA45k (50:50) nanoparticle characteristics

Polymer	Polymer Concentration (mg/mL)	Organic Solvent	Surfactant	Mean Hydrodynamic Size ± SEM (nm)	PDI ± SEM	ζ-potential ± SEM (mV)
PLGA45k (50:50)[a]	27	DCM	1% CHA	133.333 ± 5.666	0.218 ± 0.019	-73.333 ± 1.704
PLGA45k (50:50)[b]	27	DCM	1% PVA	287.767 ± 46.020	0.315 ± 0.067	-0.274 ± 0.054

[a] Data are presented as average of N=1 batch.
[b] Data are presented as average of N=3 batches.

SEM: standard error; PDI: polydispersity index

Table 2-8 Effect of EtAc and DCM on curcumin loading

Polymer	Polymer Concentration (mg/mL)	Organic Solvent	Surfactant	Drug Loading (DL) ± SEM (%)	Drug Encapsulation Efficiency (DEE) ± SEM (%)
mPEG5k-PLGA45k (50:50)[a]	20	EtAc	1% PVA	6.132 ± 1.185	47.728 ± 14.087
mPEG5k-PLGA45k (50:50)[b]	20	DCM	1% PVA	6.353 ± 0.809	47.700 ± 11.970

[a] Data are presented as average of N=9 batches.
[b] Data are presented as average of N=4 batches.

SEM: standard error

Table 2-9 Effect of 1% PVA and 1% CHA on curcumin loading

Polymer	Polymer Concentration (mg/mL)	Organic Solvent	Surfactant	Drug Loading (DL) ± SEM (%)	Drug Encapsulation Efficiency (DEE) ± SEM (%)
mPEG5k-PLGA45k (50:50)[a]	20	DCM	1% PVA	6.353 ± 0.809	47.700 ± 11.970
mPEG5k-PLGA45k (50:50)[b]	20	DCM	1% CHA	0.065 ± 0.059	0.244 ± 0.218

[a] Data are presented as average of N=4 batches.
[b] Data are presented as average of N=3 batches.

SEM: standard error

Table 2-10 Effect of PEG on nanoparticle characteristics

Polymer	Polymer Concentration (mg/mL)	Organic Solvent	Surfactant	Mean Hydrodynamic Size ± SEM (nm)	PDI ± SEM	ζ-potential ± SEM (mV)
mPEG5k-PLGA45k (50:50)[a]	20	ACN	1% F127	61.131 ± 0.745	0.121 ± 0.046	-2.691 ± 0.087
PLGA45k (50:50)[b]	5	ACN	1% F127	58.839 ± 1.975	0.148 ± 0.011	-4.975 ± 0.157

[a] Data are presented as average of N=5 batches.
[b] Data are presented as average of N=4 batches.

SEM: standard error; PDI: polydispersity index

Table 2-11 Effect of polymer concentration on mPEG5k-PLGA45k (50:50) nanoparticle characteristics

Polymer	Polymer Concentration (mg/mL)	Organic Solvent	Surfactant	Mean Hydrodynamic Size ± SEM (nm)	PDI ± SEM	ζ-potential ± SEM (mV)
mPEG5k-PLGA45k (50:50)[a]	50	ACN	1% F127	97.192 ± 8.616	0.204 ± 0.027	-2.950 ± 0.251
mPEG5k-PLGA45k (50:50)[b]	20	ACN	1% F127	61.131 ± 0.745	0.121 ± 0.046	-2.691 ± 0.087

[a] Data are presented as average of N=4 batches.
[b] Data are presented as average of N=5 batches.

SEM: standard error; PDI: polydispersity index

Table 2-12 Effect of polymer concentration on PLGA45k (50:50) nanoparticle characteristics

Polymer	Polymer Concentration (mg/mL)	Organic Solvent	Surfactant	Mean Hydrodynamic Size ± SEM (nm)	PDI ± SEM	ζ-potential ± SEM (mV)
PLGA45k (50:50)[a]	20	ACN	1% F127	145.267 ± 1.553	0.147 ± 0.031	-0.345 ± 0.152
PLGA45k (50:50)[b]	5	ACN	1% F127	58.839 ± 1.975	0.148 ± 0.011	-4.975 ± 0.157

[a] Data are presented as average of N=1 batch.
[b] Data are presented as average of N=4 batches.

SEM: standard error; PDI: polydispersity index

Table 2-13 Effect of polymer amount on nanoparticle characteristics

Polymer	Polymer Amount (mg)	Polymer Concentration (mg/mL)	Organic Solvent	Surfactant	Mean Hydrodynamic Size ± SEM (nm)	PDI ± SEM	ζ-potential ± SEM (mV)
mPEG5k-PLGA45k (50:50)[a]	50	50	ACN	1% F127	97.192 ± 8.616	0.204 ± 0.027	-2.950 ± 0.251
mPEG5k-PLGA45k (50:50)[b]	10	50	ACN	1% F127	91.063 ± 5.027	0.130 ± 0.010	-3.747 ± 0.444

[a] Data are presented as average of N=3 batches.
[b] Data are presented as average of N=1 batch.

SEM: standard error; PDI: polydispersity index

Table 2-14 Curcumin loading in mPEG5k-PLGA45k and PLGA45k nanoparticles

Polymer	Polymer Concentration (mg/mL)	Organic Solvent	Surfactant	Drug Loading (DL) ± SEM (%)	Drug Encapsulation Efficiency (DEE) ± SEM (%)
mPEG5k-PLGA45k (50:50)[a]	20	ACN	1% F127	6.004 ± 0.468	27.249 ± 2.566
PLGA45k (50:50)[b]	5	ACN	1% F127	5.266 ± 0.125	46.041 ± 20.981

[a] Data are presented as average of N=5 batches.
[b] Data are presented as average of N=4 batches.

SEM: standard error

Table 2-15 The stability of curcumin-loaded polymeric nanoparticles after 24 h.

Polymer	Polymer Concentration (mg/mL)	Organic Solvent	Surfactant	Mean Hydrodynamic Size ± SEM (nm)	PDI ± SEM	ζ-potential ± SEM (mV)
mPEG5k-PLGA45k (50:50)	20	ACN	1% F127	58.385 ± 2.289	0.063 ± 0.018	-3.748 ± 1.487
After 1 day	20	ACN	1% F127	57.447 ± 1.862	0.112 ± 0.052	-3.597 ± 1.193

Data are presented as average of N=2 batches.

SEM: standard error

Figure 2-1 Stability of curcumin-loaded polymeric nanoparticles made from the single emulsion method.

Figure 2-2 Stability of curcumin-loaded polymeric nanoparticles made from the nanoprecipitation method after 24 h.

(A) Fresh nanoparticles

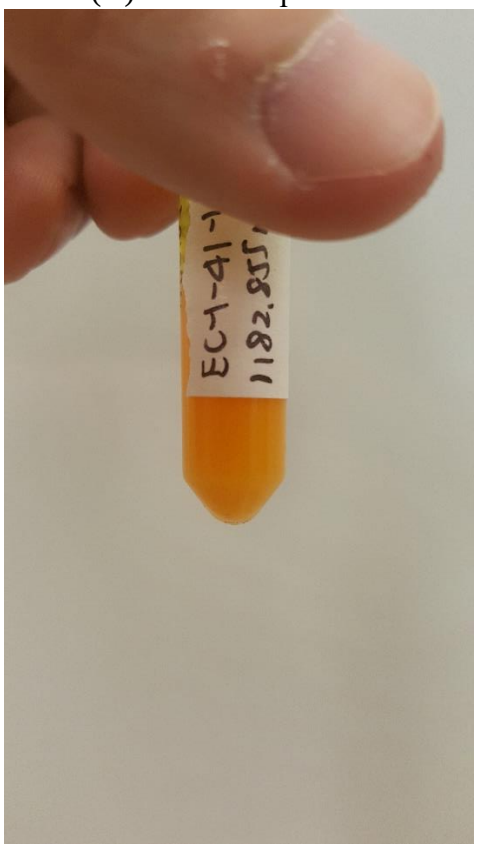

Nanoparticles after 24 h

Figure 2-3 Assessment of curcumin-loaded polymeric nanoparticle morphology using SEM.

(A) Curcumin-loaded mPEG5k-PLGA45k (50:50)

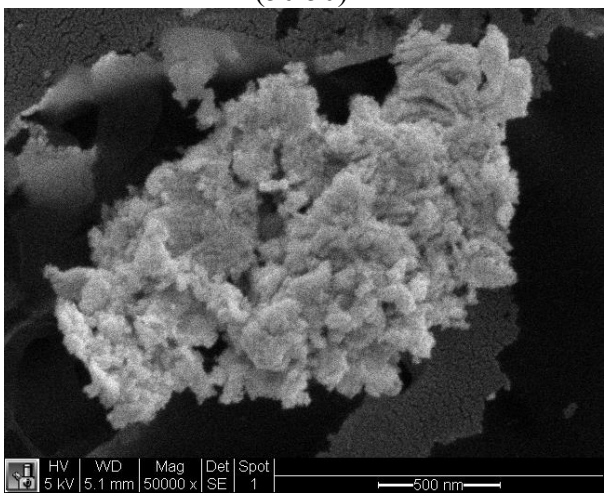

(B) Curcumin-loaded PLGA45k (50:50)

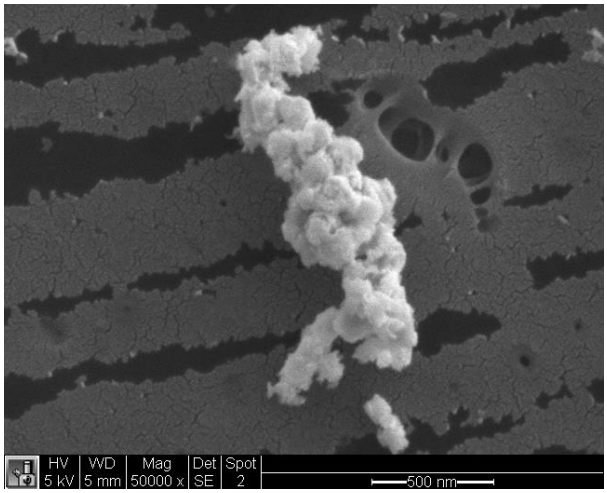

(C) Empty mPEG5k-PLGA45k (50:50)

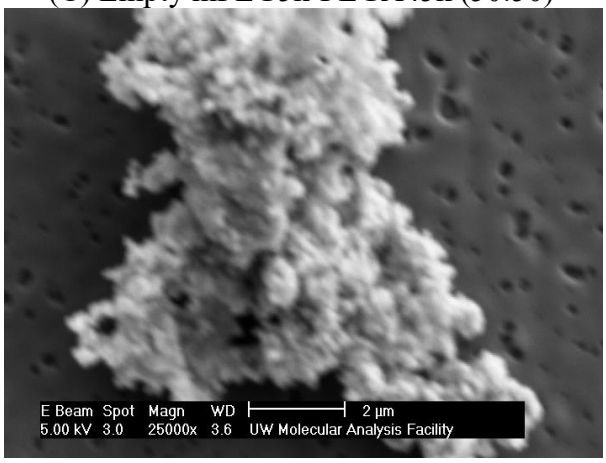

(D) Empty PLGA45k (50:50)

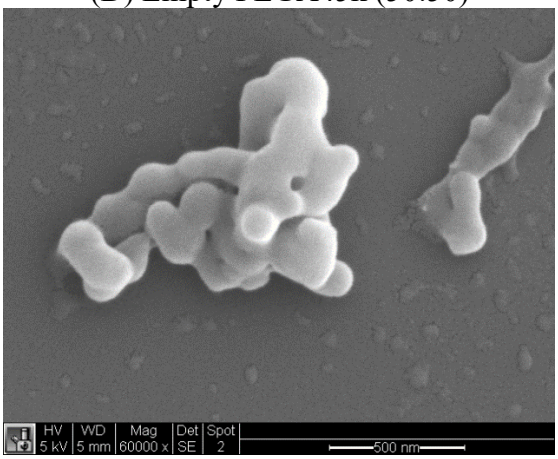

Figure 2-4 *In Vitro* curcumin release kinetics from mPEG5k-PLGA45k (50:50) and PLGA45k (50:50) nanoparticles

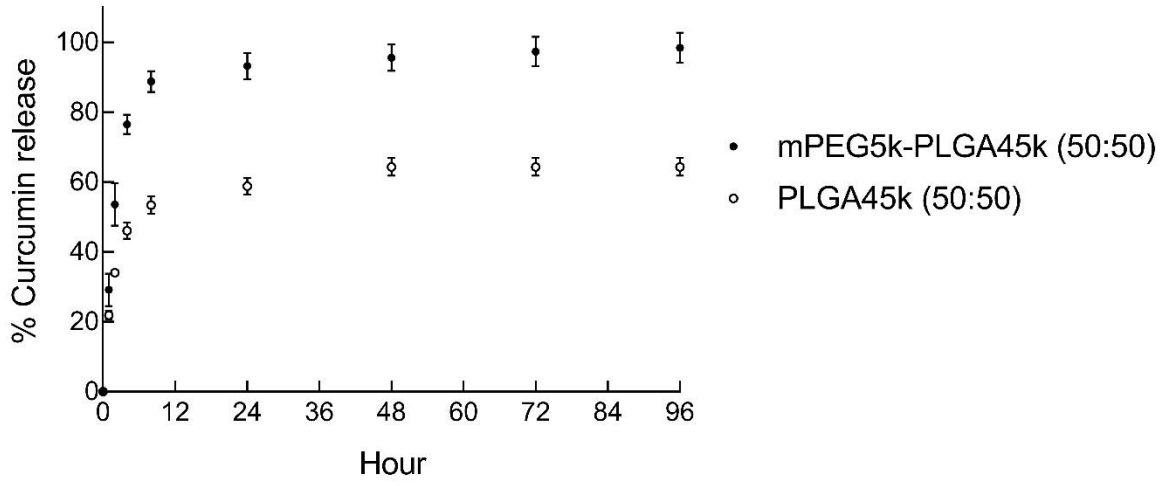

Data are presented as average of N=3 runs.

2.3 Discussion

It was recently found that with a dense PEG-coating, nanoparticles up to 114 nm with a near neutral ZP were able to diffuse within the brain parenchyma [38]. In the same study, it was shown that mPEG5k-PLGA45k (50:50) nanoparticles made by a nanoprecipitation method without surfactant satisfy the above requirements and were able to diffuse in the brain [38]. Nonetheless, only 24% of those nanoparticles were diffusing quickly. A greater fraction of diffusive nanoparticles would be desirable to reach the diseased regions in the brain and provide an effective therapeutic level. In this chapter, biodegradable mPEG5k-PLGA45k (50:50) and PLGA45k (50:50) nanoparticles were designed to satisfy the previously mentioned requirements. The morphology and curcumin release kinetics were also analyzed.

The influence of PEG layer was explored. The size of mPEG5k-PLGA45k (50:50) nanoparticles was smaller than that of PLGA45k (50:50) nanoparticles. Presumably this is due to the fact that PEG chains on the nanoparticle surface would be able to shield the PLGA core from the outside aqueous phase, and therefore a larger nanoparticle surface area could be stabilized. Both mPEG5k-PLGA45k (50:50) and PLGA45k (50:50) nanoparticles had neutral ζ-potential. This was expected because PVA tends to make nanoparticles more neutral due to the fact that it is an uncharged polymer. A similar finding was observed in one previous study where PS-COOH nanoparticle coated with PVA displayed a ζ-potential near 0 mV [44].

Another variable studied in this chapter was polymer concentration used in both the single emulsion method and the nanoprecipitation method. When using the single emulsion method, the

size of mPEG5k-PLGA45k (50:50) nanoparticles decreased by 130 nm when changing polymer concentration from 50 mg/mL to 27 mg/mL. Smaller emulsion droplets were formed with a lower polymer concentration. Interestingly, 20 mg/mL and 27 mg/mL polymer concentrations produced similarly sized nanoparticles ($p > 0.05$). One potential explanation was that these two polymer concentrations led to emulsion droplets of similar sizes, and thus resulted in similarly sized nanoparticles. Furthermore, it implied that 27 mg/mL polymer concentration could produce more nanoparticles than 20 mg/mL polymer concentration, meaning 27 mg/mL polymer concentration might be a better choice. Since the ζ-potential was not significantly impacted by different polymer concentrations, and a smaller size nanoparticle was preferred, 27 mg/mL polymer concentration was selected for future nanoparticle formulation. When using the single emulsion method, the size of the PLGA45k (50:50) nanoparticle decreased 15 nm when changing polymer concentration from 27 mg/mL to 10 mg/mL; however, the difference was not significant ($p > 0.05$).

When changing polymer concentration from 50 mg/mL to 20 mg/mL using the nanoprecipitation method, the size of the mPEG5k-PLGA45k (50:50) nanoparticles decreased 35 nm ($p < 0.05$). In this case, a higher polymer concentration led to a larger size polymer droplet and therefore gave rise to a larger size nanoparticle. The same trend was seen in the size of the PLGA45k (50:50) nanoparticle—a higher polymer concentration also brought about a larger size nanoparticle. ζ-potential was not significantly influenced by the polymer concentration and remained near neutral ($p > 0.05$ for mPEG5k-PLGA45k (50:50) nanoparticle).

mPEG5k-PLGA45k (50:50) and PLGA45k (50:50) nanoparticles made by the nanoprecipitation method had a smaller size than those made by the single emulsion method. The size difference was

likely caused by the use of a more water-miscible organic solvent, acetone, in the nanoprecipitation method and a less water-miscible organic solvent, DCM and EtAc, in the single emulsion method. A more water-miscible organic solvent would result in a decrease in the surface tension of the polymer droplet in the aqueous phase and further influence the nanoparticle's size during solvent diffusion into the aqueous phase [45]. When we look at the solubility of the organic solvent in water, we can notice acetone is completely soluble in water, whereas EtAc and DCM are poorly miscible. Due to ACN's free miscibility with water, the surface tension of the polymer droplet was the lowest and thus caused the smallest size nanoparticles. Since EtAc and DCM had less solubility in the water, they resulted in a larger size nanoparticle than that formulated from acetone. ζ-potential was not significantly influenced by the organic solvent used in the formulation. Since the nanoprecipitation method produced a lower size nanoparticle than that made from the single emulsion method, the nanoprecipitation method was favored because a smaller size nanoparticle was preferred for drug delivery to the brain.

The influence of different organic solvents, DCM and EtAc, on mPEG5k-PLGA45k (50:50) and PLGA45k (50:50) nanoparticles made from the single emulsion method was investigated. As discussed previously, the organic solvent's solubility in water would influence the size of the nanoparticle. Since EtAc is more miscible with water, it gave rise to a lower surface tension of the polymer droplet in the aqueous phase than that of the polymer droplet made from DCM, it resulted in a smaller size nanoparticle than that made from DCM. This explanation applied to both mPEG5k-PLGA45k (50:50) and PLGA45k (50:50) nanoparticles ($p < 0.05$ for mPEG5k-PLGA45k (50:50) nanoparticle). Different organic solvents did not greatly influence the ζ-potentials of both mPEG5k-PLGA45k (50:50) and PLGA45k (50:50) nanoparticles ($p > 0.05$ for

mPEG5k-PLGA45k (50:50) nanoparticle). Furthermore, both DCM and EtAc had no significant influence on the curcumin loading for the mPEG5k-PLGA45k (50:50) nanoparticle ($p > 0.5$). However, EtAc was not a good organic solvent in this research. A short while after the curcumin and the polymer were dissolved in EtAc, the polymer and curcumin would precipitate out from EtAc, and thereby DCM was the one selected for future nanoparticle formulation if one were to use the single emulsion method.

The effect of different surfactants, 1% (w/v) PVA and 1% (w/v) CHA, was also one of the parameters investigated in this research. The sizes of both the mPEG5k-PLGA45k (50:50) and PLGA45k (50:50) nanoparticles made from the single emulsion method were decreased when switching from 1% (w/v) PVA to 1% (w/v) CHA by 50 nm and 150 nm respectively ($p < 0.05$ for the mPEG5k-PLGA45k (50:50) nanoparticles). One potential explanation is PVA is much harder to be washed away from the surface of the nanoparticle than CHA. This is due to the fact that PVA has a much higher molecular weight, and thereby, the sizes of the mPEG5k-PLGA45k (50:50) and PLGA45k (50:50) nanoparticles all increased when they were made from 1% (w/v) PVA. Moreover, PVA is a more adhesive polymer than CHA, and nanoparticles made from 1% (w/v) PVA could aggregate together and cause a higher PDI ($p < 0.05$ for mPEG5k-PLGA45k (50:50) nanoparticle). However, 1% (w/v) CHA resulted in a much lower curcumin loading for the mPEG5k-PLGA45k (50:50) nanoparticle ($p < 0.05$). Loss of CHA during collection and washing could increase curcumin release from the nanoparticle. On the other hand, because PVA was harder to be washed away from the nanoparticle, it protected and prevented curcumin from releasing from the nanoparticle making it as a better surfactant than CHA. As a result, 1% (w/v) PVA was selected for future nanoparticle formulation, when using the single emulsion method.

The stability of the nanoparticle was investigated in this research, as well. Both mPEG5k-PLGA45k (50:50) and PLGA45k (50:50) nanoparticles made from the single emulsion method were unstable. Nanoparticles, made from the nanoprecipitation method had better stability and decreased precipitation in a 24 h window. The size, PDI, and ζ-potential all remained unchanged after 24 h. However, nanoparticles should be stable for a longer time period and therefore, longer stability studies will be explored in future work.

The effect of amount of polymer used to formulate nanoparticle was also investigated. The PDI of the nanoparticle would increase when more polymer (same polymer concentration) was used to formulate the nanoparticle, but the size and ζ-potential of the nanoparticle remained unchanged. Presumably, more polymer lead to an increase in polymer per polymer droplet, which led to the polymer droplet more easily aggregating together and thus caused a higher PDI.

The curcumin release kinetics from both mPEG5k-PLGA45k (50:50) and PLGA45k (50:50) nanoparticles was also analyzed by the HPLC. Both mPEG5k-PLGA45k (50:50) and PLGA45k (50:50) nanoparticles did provide a sustained curcumin release over 24 to 48 h. Nearly 100% curcumin was released from mPEG5k-PLGA45k (50:50) nanoparticle, while only around 60% to 65% curcumin was released from PLGA45k (50:50) nanoparticle. The different release kinetics could be due to curcumin being encapsulated deep inside the core of PLGA45k (50:50) nanoparticles, leading to some curcumin remaining trapped inside the PLGA45k (50:50) nanoparticle after 96 h. Therefore, we will need to evaluate PLGA45k (50:50) nanoparticle degradation time (typically a few months are needed) to see if the percent of curcumin released

from PLGA45k (50:50) nanoparticles reaches 100%. On the other hand, since mPEG5k-PLGA45k (50:50) nanoparticles have a PEG layer, it is possible most curcumin was encapsulated on the surface of the PLGA core rather than inside the PLGA core, and thus more curcumin was released from the mPEG5k-PLGA45k (50:50) nanoparticles more quickly.

Overall, in this chapter, the nanoprecipitation method with ACN as the organic solvent and 1% (w/v) F127 as the surfactant could produce comparable and similar results both in the size (sub-60 nm) and PDI for mPEG5k-PLGA45k (50:50) and PLGA45k (50:50) nanoparticles. Both nanoparticles had nearly neutral ζ-potential, which met the requirements as reported [38] in order to make sure nanoparticles would have the ability to diffuse within the brain parenchyma.

2.4 Conclusion

The single emulsion method and nanoprecipitation method were tried and optimized to create small, uniform and near neutral curcumin-loaded mPEG5k-PLGA45k (50:50) and PLGA45k (50:50) nanoparticles. The single emulsion method with either EtAc or DCM as the organic solvent and either 1% (w/v) PVA or 1% (w/v) CHA as the surfactant had difficulty in creating stable or high curcumin loaded nanoparticles. By the nanoprecipitation method with ACN as the organic solvent and 1% (w/v) F127 as the surfactant, we were able to engineer and create stable mPEG5k-PLGA45k (50:50) and PLGA45k (50:50) nanoparticles that had comparable results on the size, PDI, ζ-potential and curcumin loading. These nanoparticles provided a sustained curcumin release over 24 to 48 h. By changing the polymer concentration, we could easily tune the size of the nanoparticle. In order to demonstrate these nanoparticles provide a potential curcumin delivery

platform for treatment of HIE, nanoparticles should have the ability to cross the BBB and to move within the brain parenchyma and will be discussed in the next chapter.

Chapter 3 The Effective Diffusivity and Biodistribution of Nanoparticles in Neonatal Rat Brain

3.1 Materials and Methods

3.1.1 Polymer Labeling with a Fluorescence Dye

PLGA45k (50:50) polymer and mPEG5k-PLGA45k (50:50) copolymer were labeled with AlexaFluor 647 NHS Ester (Succinimidyl Ester) fluorescence dye (AF647; Life Technologies, Carlsbad, CA) as described previously [46]. Briefly, the polymer was first dissolved in DCM. Dissolved p-nitrophenyl chloroformate (PNCF; Sigma-Aldrich, St Louis, MO) in DCM at 10 mg/mL. The polymer was activated by adding PNCF and then pyridine (Sigma-Aldrich, St Louis, MO). The reaction was carried out for 3 h under constant stirring. The activated polymers were precipitated in cold diethyl ether (Sigma-Aldrich, St Louis, MO) and collected by a tabletop centrifuge at 1,000 xg and 4ºC for 2 minutes and lyophilized overnight. The lyophilized activated polymer and the AF647 dye were dissolved in dimethylformamide (DMF; Sigma-Aldrich, St Louis, MO), and trimethylamine (TEA; Sigma-Aldrich, St Louis, MO) was added immediately to the polymer dye mixture. The reaction was carried out for 4 h under constant stirring. The fluorescently labeled polymer were precipitated in cold diethyl ether two or three times and collected by a tabletop centrifuge at 1,000 xg and 4ºC for 2 minutes and lyophilized overnight.

3.1.2 Nanoparticle Preparation

AF647-labeled or unlabeled or curcumin-loaded mPEG5k-PLGA45k (50:50) and PLGA45k (50:50) nanoparticles were prepared by either the nanoprecipitation method or the single emulsion method similar as described previously in **Section 2.1.1.1** and **2.1.1.2**. The organic solvent and the surfactant were ACN and 1% (w/v) F127 respectively for the nanoprecipitation method and DCM and 1% (w/v) PVA respectively for the single emulsion method. Nanoparticles were all used immediately.

3.1.3 Nanoparticle Characterization

Nanoparticle characterization was performed as described in **Section 2.1.2**.

3.1.4 *Ex Vivo* Neonatal Postnatal Day 12 (P12) Rat Brain Slices Preparation

All animal experiments were carried out at the University of Washington Chemical Engineering Department or School of Medicine following National Institutes of Health guidelines and local Institutional Animal Care and Use Committee (IACUC) regulations. Briefly, P12 Sprague-Dawley rats were euthanized with pentobarbital. Then the brain was rapidly removed and cut into 300 μm thick slices using a rat brain chopper (Cavey Laboratory Engineering Co. Ltd., England). The chopper and razor blades were sprayed with 70% (v/v) ethanol prior to use.

3.1.5 Multiple Particle Tracking in Neonatal P12 rat brain slices

The transport rate of nanoparticles was determined by analyzing the trajectory of the nanoparticle as described previously [38]. Briefly, the particle trajectories in the brain tissue slices were recorded by an inverted research microscope (Eclipse Ti, Nikon, Tokyo, Japan) equipped with a 40x oil-immersion objective lens (N.A., 1.30). The cortex and midbrain regions without tissue shift were imaged. Movies were captured by Nikon NIS-Elements Confocal software at a temporal resolution of 3.95 frames per second (FPS) for 22.54 seconds. Trajectories of >500 nanoparticles were analyzed for each sample using ImageJ, and the coordinates of particle centroids were used to calculate the time-average mean squared displacement (MSD), defined as :

$$< \Delta r^2(\tau) >= [x(t+\tau) - x(t)]^2 + [y(t+\tau) - y(t)]^2$$

where τ is the time scale or time lag, x and y are the nanoparticle's x-, y-coordinates at a given time, respectively, and t is the initial time of acquisition. Distributions of MSDs and effective diffusivities (D_{eff}) were calculated as described previously [47]. Moreover, MSDs as a function of τ can be expressed as:

$$MSD = 4D_{eff}\tau^{\alpha}$$

When this relationship is plotted on a log-log scale, α represents the slope of the curve and is a unitless parameter that measures the extent of impediment to nanoparticle diffusion [48].

3.1.6 Brain Localization of AF647-labeled mPEG5k-PLGA45k (50:50) in Neonatal P7 rat

3.1.6.1 Neonatal P7 HIE rat model preparation

All animal experiments were carried out at the University of Washington Chemical Engineering Department or School of Medicine following National Institutes of Health guidelines and local Institutional Animal Care and Use Committee (IACUC) regulations. Sprague-Dawley P7 rats were used. For the HI groups, hypoxia was induced by left carotid artery ligation surgery and ischemia was induced by a reduced-oxygen environment. Briefly, the left carotid artery ligation surgery was 5-10 mins to induce ischemia. The rats would recover in the home cage for 30 min. After the recovery, the rats were placed in a reduced-oxygen container, 8% oxygen plus 92% nitrogen, to induce hypoxia for 2.5 h.

3.1.6.2 Brain Localization of AF647-labeled mPEG5k-PLGA45k (50:50) in Neonatal P7 rat Procedure

All animal experiments were carried out at the University of Washington Chemical Engineering Department or School of Medicine following National Institutes of Health guidelines and local Institutional Animal Care and Use Committee (IACUC) regulations. There were three groups and three Sprague-Dawley P7 rats were used for each group. The three groups included HI group 1 (rats with HI injury), HI group 2 (rats with HI injury) and control group (rats without HI injury). 30 minutes after the hypoxia, HI group 1 and the control group were intraperitoneally (IP) injected with AF647-labeled mPEG5k-PLGA45k (50:50) nanoparticle with 50 mg/kg dose and 0.5 mL of a 300 mg/mL solution of fluorescein isothiocyanate-dextran (dex-FITC, average MW 3000-5000;

Sigma-Aldrich, St Louis, MO) made in saline. At 30 min after HI, HI group 2 was IP injected with only AF647-labeled mPEG5k-PLGA45k (50:50) nanoparticles. After 24 h, all rats were euthanized, the pups were perfused with saline, and the brains were removed and placed in formalin. Cryosectioning was performed, as described in **Section 3.1.6.3**. Each section was stained with 4',6-diamidino-2-phenylindole (DAPI; Life Technologies, Carlsbad, CA) and imaged by an inverted research microscope equipped with a 40x oil-immersion objective lens (N.A., 1.30) and a 20x objective lens (N.A., 0.75).

3.1.6.3 Cryostat Section

All animal experiments were carried out at the University of Washington Chemical Engineering Department or School of Medicine following National Institutes of Health guidelines and local Institutional Animal Care and Use Committee (IACUC) regulations. Briefly, P7 Sprague-Dawley HI or healthy rats were euthanized with pentobarbital. Afterward, the rats were perfused with 1x PBS. Then the brain was rapidly removed and fixed in 10% (v/v) Buffered Formalin Phosphate for one day. The fixed brain was immersed in 15% (w/v) sucrose gradient for two days and then 30% (w/v) sucrose gradient for two days. The brain was sectioned into 30 μm thick sections using a Leica CM1950 cryostat section (Leica Biosystems Inc. Buffalo Grove, IL).

3.1.7 Distribution of Curcumin Delivered by mPEG5k-PLGA45k (50:50) Nanoparticle in Neonatal P7 HIE Rats

3.1.7.1 Neonatal P7 HIE rat model preparation

All animal experiments were carried out at the University of Washington Chemical Engineering Department or School of Medicine following National Institutes of Health guidelines and local Institutional Animal Care and Use Committee (IACUC) regulations. Three Sprague-Dawley P7 HIE rats were studied and prepared as described in **Section 3.1.6.1**.

3.1.7.2 Tissue homogenization

Briefly, 500 ± 15 mg of frozen tissue were dissected and homogenized in 1 mL 1x PBS using a homogenizer. Suspensions were centrifuged at 15,000 rpm for 15 minutes at 4ºC using a microcentrifuge. The resulting supernatants were separated and run on a UV-vis spectroscometer to measure curcumin content.

3.1.7.3 Distribution of curcumin delivered by mPEG5k-PLGA45k (50:50) nanoparticle in neonatal P7 HIE rats procedure

All animal experiments were carried out at the University of Washington Chemical Engineering Department or School of Medicine following National Institutes of Health guidelines and local Institutional Animal Care and Use Committee (IACUC) regulations. 30 minutes after hypoxia, rats (n =3) were IP injected with curcumin-loaded mPEG5k-PLGA45k (50:50) nanoparticle with 10 mg/kg dose. After 24 h, the rats were euthanized with pentobarbital. Brains, kidneys, livers and

serum were collected, homogenized and measured curcumin content as described in **Section 3.1.7.2**.

3.2 Results

3.2.1 Effective Diffusivity of AF647-labeled mPEG5k-PLGA45k (50:50) and PLGA45k (50:50) Nanoparticles in *Ex Vivo* Neonatal P12 Rat Brain Slices

The ensemble-averaged trajectories of AF647-labeled mPEG5k-PLGA45k (50:50) and PLGA45k (50:50) nanoparticles in cortex and midbrain regions were compared and are shown in **Figure 3-1**. The trajectories of AF647-labeled mPEG5k-PLGA45k (50:50) nanoparticle was longer than that of AF647-labeled PLGA45k (50:50) nanoparticle independent of brain region. Moreover, mPEG5k-PLGA45k (50:50) and PLGA45k (50:50) nanoparticles both had better mobility in the cortex region than in the midbrain. The ensemble-averaged MSDs and distribution of the logarithmic D_{eff} at a time scale of 1 s of AF647-labeled mPEG5k-PLGA45k (50:50) and PLGA45k (50:50) nanoparticles in cortex region are shown in **Figure 3-2** and **Figure 3-3**. The ensemble-averaged MSD of mPEG5k-PLGA45k (50:50) nanoparticle was larger than that of PLGA45k (50:50) nanoparticle. The diffusivity of mPEG5k-PLGA45k (50:50) nanoparticle represented a mobile nanoparticle. The diffusivity of PLGA45k (50:50) nanoparticle, on the other hand, displayed an immobile nanoparticle, but the result from PLGA45k (50:50) nanoparticle was not significant since only 7 nanoparticles were captured. More experiments are needed for this section in the future in order to have a more significant and reliable result and a better sense of diffusion in the P12 rat brain.

3.2.2 Blood-brain Barrier Impairment in the Neonatal P7 rats

BBB impairment was investigated in the HI model, as introduced in **Section 3.1.6**. Dex-FITC generally is used as a fluorescent probe to study cell processes such as cell permeability and to study mechanisms of biomolecular delivery. In this study, dex-FITC was used to demonstrate the BBB impairment in the HI rats. Images of dex-FITC's extravasation to the injured hippocampus and control hippocampus are shown in **Figure 3-4**. Some dex-FITC extravasated in the injured hippocampus region; nonetheless, no dex-FITC was in the control hippocampus region, demonstrating that BBB impairment only occurred in the presence of injury in the HI rats.

3.2.3 Brian Localization of AF647-labeled mPEG5k-PLGA45k (50:50) Nanoparticle in the Neonatal P7 Rats

Nanoparticle passage across the BBB was investigated in the HI rats. As shown in **Figure 3-5**, some AF647-labeled mPEG5k-PLGA45k (50:50) nanoparticles were seen in the injured hippocampus, while no AF647-labeled mPEG5k-PLGA45k (50:50) nanoparticles were seen in the control hippocampus. This demonstrates mPEG5k-PLGA45k (50:50) nanoparticles are able to cross the impaired BBB in the HI brain.

3.2.4 Distribution of Curcumin Delivered by mPEG5k-PLGA45k (50:50) Nanoparticle in Neonatal P7 HIE Rats

Incorporation of curcumin into a nanoparticle platform is our strategy to deliver curcumin across the BBB. The quantified result of the distribution of curcumin delivered by mPEG5k-PLGA45k (50:50) nanoparticles in neonatal P7 HI rats is shown in **Figure 3-6**. Curcumin delivered by

mPEG5k-PLGA45k (50:50) nanoparticles could accumulate in the HI brain. A large amount of curcumin was measured in the liver and kidney. Nanoparticles larger than 100 nm would go through first-pass metabolism, and accumulate in the liver. After the curcumin was released from the nanoparticle, it would be cleared by the kidney.

Figure 3-1 The ensemble-averaged trajectories of AF647-labeled mPEG5k-PLGA45k (50:50) nanoparticle in the (A) cortex and (B) midbrain regions and PLGA45k (50:50) nanoparticle in the (C) cortex and (D) midbrain regions. Each ensemble-averaged trajectory was averaged by two videos per sample.

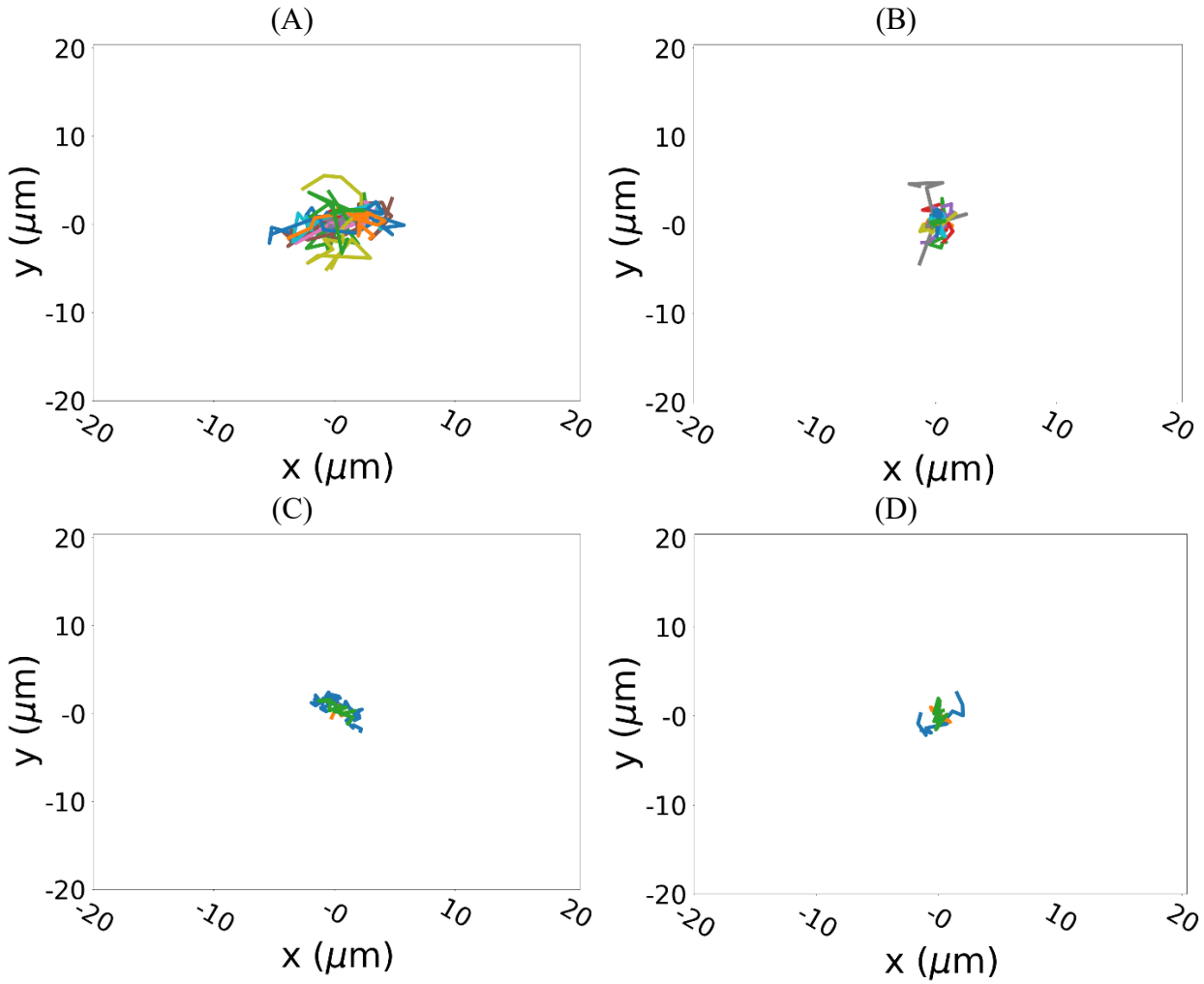

Figure 3-2 The ensemble-averaged MSDs of (A) AF647-labeled mPEG5k-PLGA45k (50:50) and (B) PLGA45k (50:50) nanoparticles in the cortex region

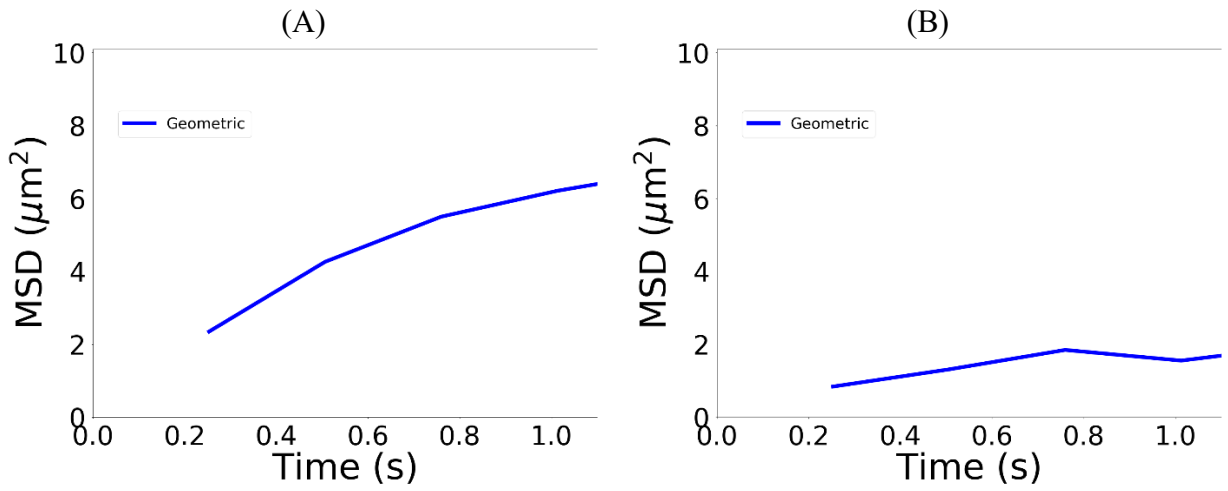

Figure 3-3 The distribution of the logarithmic D_{eff} at a time scale of 1 s of (A) AF647-labeled mPEG5k-PLGA45k (50:50) and (B) PLGA45k (50:50) nanoparticles in the cortex region.

(A)

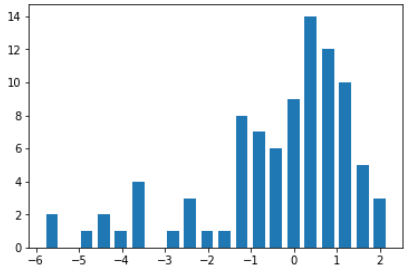

logarithm of the diffusion coefficients (μm^2) at τ = 1s

(B)

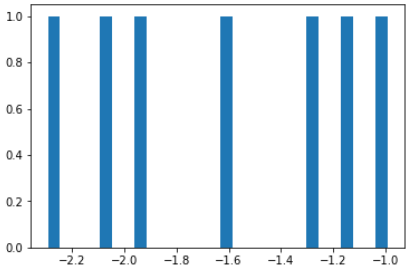

logarithm of the diffusion coefficients (μm^2) at τ = 1s

Figure 3-4 Images of dex-FITC's extravasation to the (A) injured hippocampus and the (B) control hippocampus. Blue as DAPI. Green as dextran-FITC. In the control hippocampus, dextran-FITC is localized in the ventricles, whereas dextran-FITC has extravasated into the parenchyma in the HI brain.

(A) (B)

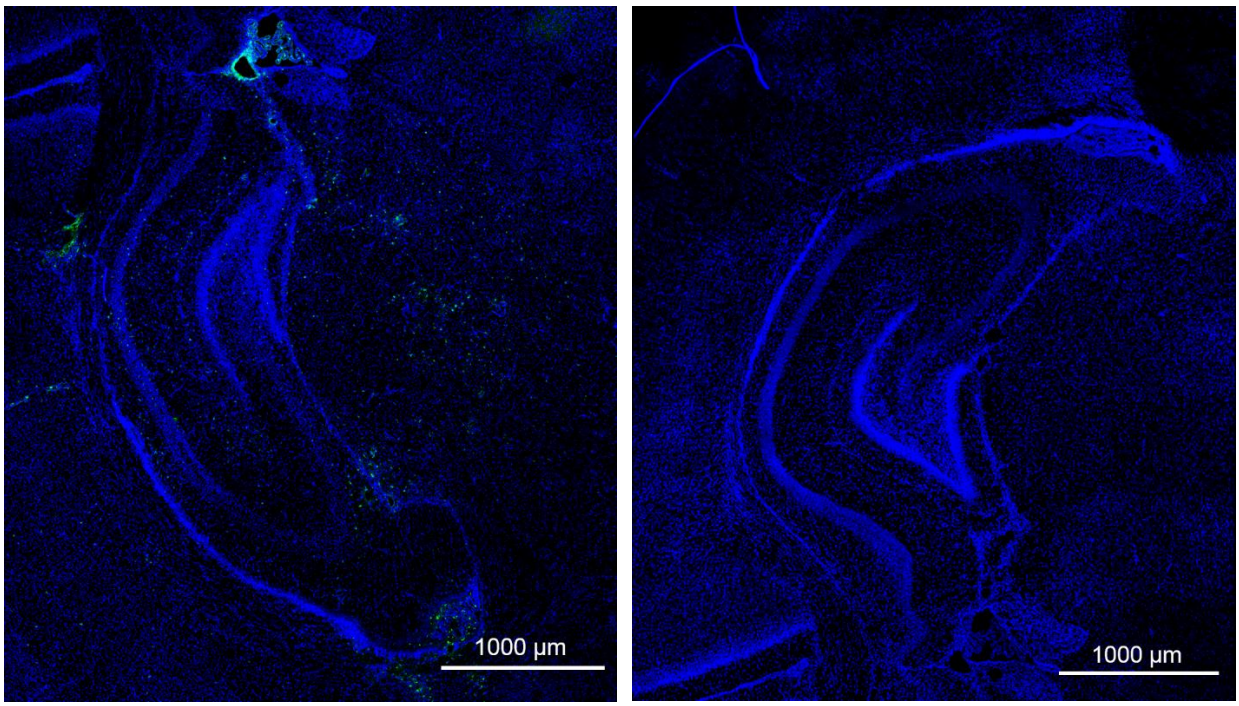

Figure 3-5 Brain localization of AF647-labeled mPEG5k-PLGA45k (50:50) nanoparticles in the (A) injured hippocampus of the HI brain and the (B) control hippocampus of a healthy pup. Blue is nuclei stained by DAPI. Red is AF647-labeled nanoparticle.

(A) (B)

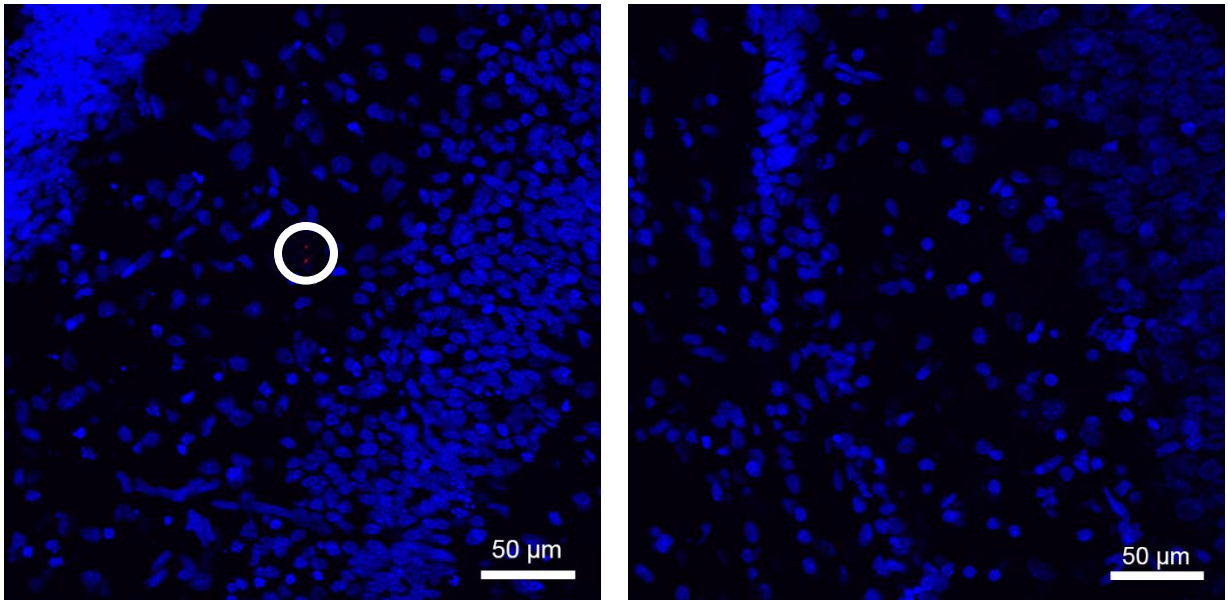

Figure 3-6 Distribution of curcumin delivered by mPEG5k-PLGA45k (50:50) nanoparticles in neonatal P7 HIE rats.

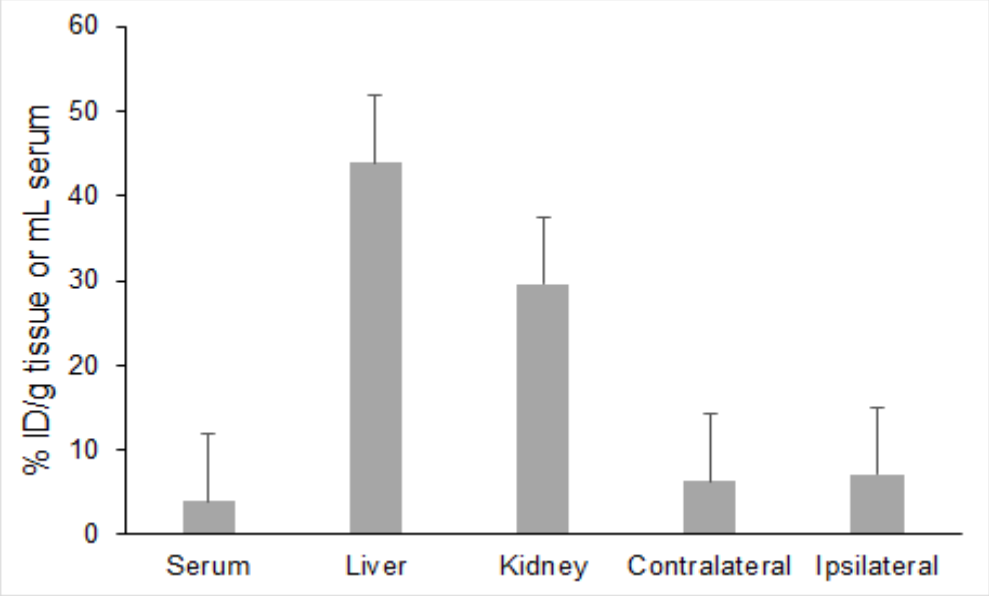

3.3 Discussion

Surfactant F127 used in this research is commonly used as a surface coating to enhance nanoparticle passage across the BBB; however, the effect of F127 on mPEG5k-PLGA45k (50:50) and PLGA45k (50:50) nanoparticles' diffusion within the brain parenchyma has not yet been fully understood. Once nanoparticles cross the BBB, the ability of the nanoparticle to diffuse to the hippocampus is still unknown. Furthermore, whether curcumin delivered by mPEG5k-PLGA45k (50:50) nanoparticle accumulates in the hippocampus is not fully understood. Therefore, in this chapter, curcumin-loaded mPEG5k-PLGA45k (50:50) and PLGA45k (50:50) nanoparticles and AF647-labelled mPEG5k-PLGA45k (50:50) and PLGA45k (50:50) nanoparticles were formulated to investigate nanoparticle diffusion, uptake, and distribution in the rat brain. The effective diffusivities in the neonatal P12 rat brain *ex vivo* were analyzed. Brain localization of mPEG5k-PLGA45k (50:50) nanoparticles in the neonatal P7 rat brain and the distribution of curcumin delivered by mPEG5k-PLGA45k (50:50) nanoparticles in the neonatal P7 HIE rats were investigated.

The ensemble-averaged trajectory of AF647-labeled mPEG5k-PLGA45k (50:50) nanoparticle was longer than that of AF647-labeled PLGA45k (50:50) nanoparticle in the cortex region. The ensemble-averaged MSD of mPEG5k-PLGA45k (50:50) nanoparticle was also larger than that of PLGA45k (50:50) nanoparticle. The diffusivity of mPEG5k-PLGA45k (50:50) nanoparticle represented a mobile nanoparticle. The diffusivity of PLGA45k (50:50) nanoparticle, however, displayed an immobile nanoparticle. AF647-labeled mPEG5k-PLGA45k (50:50) and AF647-labeled PLGA45k (50:50) nanoparticles had similar and comparable results in the size, PDI, and

ζ-potential, suggesting they should have similar diffusive abilities in the brain tissue. However, once nanoparticles get into the brain microenvironment, F127 might desorb from the nanoparticle surface, exposing the hydrophonic PLGA45k (50:50) nanoparticle surface, leading to aggregation or interaction with proteins in the brain microenvironment. Even if F127 desorbed from the mPEG5k-PLGA45k (50:50) nanoparticle surface, the PEG layer would still stabilize the nanoparticle, and minimize and prevent non-specific protein absorption and interactions within biological medium.

In this model, the hippocampus is the area most susceptible to injury. As shown in **Figure 3-4,** some dex-FITC could be seen in the HI hippocampus while no dex-FITC was seen in the control hippocampus, demonstrating the BBB in the HI hemisphere was impaired. We also did see some AF647-labeled mPEG5k-PLGA45k (50:50) nanoparticle in the HI hippocampus region while no AF647-labeled mPEG5k-PLGA45k (50:50) nanoparticle was seen in the control hippocampus as shown in **Figure 3-5**. This shows the ability of mPEG5k-PLGA45k (50:50) nanoparticles to penetrate the impaired BBB, which can increase curcumin delivery into the brain.

Due to the fact that mPEG5k-PLGA45k (50:50) nanoparticle was able to penetrate the impaired BBB, the distribution of curcumin delivered by mPEG5k-PLGA45k (50:50) nanoparticle in the various organs in the neonatal HIE rats was further analyzed and quantified. Based on our preliminary study, we did see curcumin accumulation in the brain when delivered by a nanoparticle platform. However, a significant portion of curcumin was measured in the liver and kidney. Nanoparticles larger than 100nm would first be removed by the liver, and after the curcumin was released from the nanoparticle, it would be removed by the kidney. In the future, we will increase

animal numbers to account for injury variability, and we will also include one control group treated with free curcumin to have a better sense of the difference in the distribution of curcumin delivered with or without the help of the nanoparticle in various organs of the neonatal P7 HIE rats. Lastly, we will utilize our optimized nanoprecipitation nanoparticle formulation (~50nm, near neutral surface charge) for future biodistribution studies.

Overall, in this chapter, we demonstrated mPEG5k-PLGA45k (50:50) nanoparticle could diffuse within the brain microenvironment and curcumin-loaded mPEG5k-PLGA45k (50:50) nanoparticle is a feasible platform to deliver curcumin across the impaired BBB in the neonatal P7 HI rats. In the future, more diffusion studies with increased animal numbers need to be completed. To account for model variability, at least twenty rats are needed to have a better sense of average mPEG5k-PLGA45k (50:50) nanoparticle uptake and diffusion in the neonatal rat brain.

3.4 Conclusion

In chapter 2, we demonstrated the nanoprecipitation method could successfully formulate stable curcumin-loaded mPEG5k-PLGA45k (50:50) and PLGA45k (50:50) nanoparticles with sub-60 nm in size, near neutral ζ-potential, fine curcumin loading and a sustained curcumin release over 24 to 48 h. In this chapter, we demonstrated mPEG5k-PLGA45k (50:50) nanoparticles could diffuse within the brain parenchyma rapidly. We also showed that mPEG5k-PLGA45k (50:50) nanoparticle could cross the impaired BBB to reach the hippocampus and successfully deliver curcumin in the neonatal P7 rat brains. These data demonstrated mPEG5k-PLGA45k (50:50) nanoparticles could be a delivery platform to overcome curcumin's current therapeutic limitations.

In order to demonstrate curcumin-loaded nanoparticles could provide a neuroprotection and reduce neuronal injury, its efficacy should be investigated and will be discussed in the next chapter.

Chapter 4 Preliminary Efficacy Study of Curcumin-loaded mPEG-PLGA Nanoparticles in Neonatal Hypoxic-Ischemic Encephalopathy Rat Model

4.1 Materials and Methods

4.1.1 Nanoparticle Preparation

Curcumin-loaded mPEG5k-PLGA45k (50:50) nanoparticles were formulated by the single emulsion method as similarly described in **Section 2.1.1.2**. mPEG5k-PLGA45k (50:50) polymer was dissolved in EtAc with 10% target curcumin loading. The solution was then added into 5 mL 0.5% (w/v) PVA surfactant immediately followed by sonication using a probe sonicator in a water-ice bath for 1 minute at 30% amplitude (1 second on/1 second off). The emulsified solution was immediately poured into 25 mL 1% (w/v) PVA surfactant, and was stirred magnetically at speed 700 rpm for 3 hours. The organic solvent was further removed by rotary evaporator under reduced pressure, 15 mbar, at 4ºC for 30 minutes. Nanoparticles were collected and washed twice by normal centrifugation by DI water. Nanoparticles were then suspended in 1x PBS and used immediately.

4.1.2 Nanoparticle Characterization

Nanoparticle characterization was performed as described in **Section 2.1.2**.

4.1.3 Neonatal P7 HIE rat model preparation

All animal experiments were carried out at the University of Washington Chemical Engineering Department or School of Medicine following National Institutes of Health guidelines and local Institutional Animal Care and Use Committee (IACUC) regulations. Briefly, P7 Sprague-Dawley rats were used. Hypoxia was induced by left carotid artery ligation surgery. Ischemia was induced by a reduced-oxygen environment. Briefly, all the rats received left carotid artery ligation within 5-10 mins to induce ischemia. The rats would recover in the home cage for 30 min. After the recovery, the rats were placed in a reduced-oxygen container, 8% oxygen plus 92% nitrogen, to induce hypoxia for 2.5 h.

4.1.4 Experimental Procedure

All animal experiments were carried out at the University of Washington Chemical Engineering Department or School of Medicine following National Institutes of Health guidelines and local Institutional Animal Care and Use Committee (IACUC) regulations. Two experimental groups included a nanocurcumin-treated group and a saline treated group. Each group included 8 HI rats. 30 minutes after the hypoxia, the rats received either curcumin-loaded nanoparticle with 25 mg/kg dose of curcumin or a volume equivalent dose of saline. After 24 h, pups received a second dose group of curcumin-loaded nanoparticle with 25 mg/kg dose of curcumin or saline. All the rats were euthanized with pentobarbital at P14. Afterward, the rats were perfused with 1x PBS. The brain was rapidly removed and evaluated curcumin's efficacy on providing neuroprotection to the HI brain using area loss assessment [49] and injury severity score [50].

4.2 Results

4.2.1 Area Loss Assessment

Percent area loss assessment of the injured hemisphere was done to evaluate curcumin-loaded nanoparticle's therapeutic efficacy on providing neuroprotection to the neonatal HI rats. The evaluation was carried out as described in reference [51]. The result is shown in **Figure 4-1**. We could notice the rats treated with curcumin-loaded nanoparticle did not have better neuroprotection compared with the rats treated with saline.

4.2.2 Injury Severity Score

Injury severity score was also done to evaluate curcumin-loaded nanoparticle's therapeutic efficacy on supplying neuroprotection to the neonatal HI rats. The evaluation was carried out as described in reference [52]. The result is shown in **Figure 4-2**. We could notice the rats treated with curcumin-loaded nanoparticle did have a trend towards a lower average injury score than that of the rats treated with saline.

Figure 4-1 Curcumin’s efficacy evaluation by percent area loss

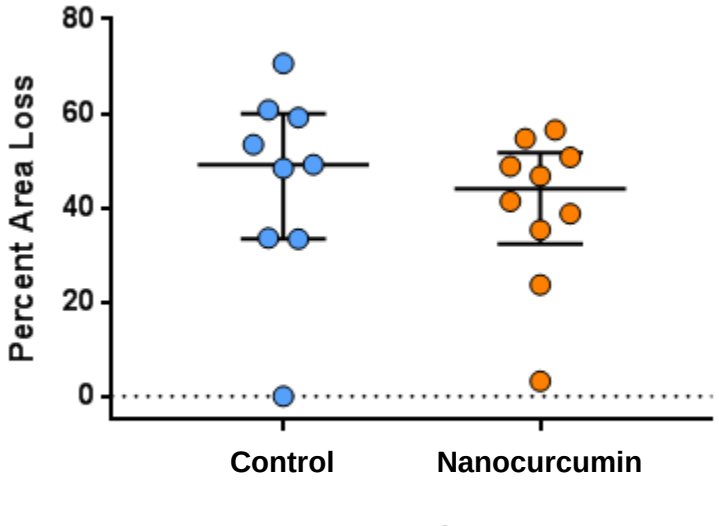

Figure 4-2 Curcumin's efficacy evaluation by injury severity score

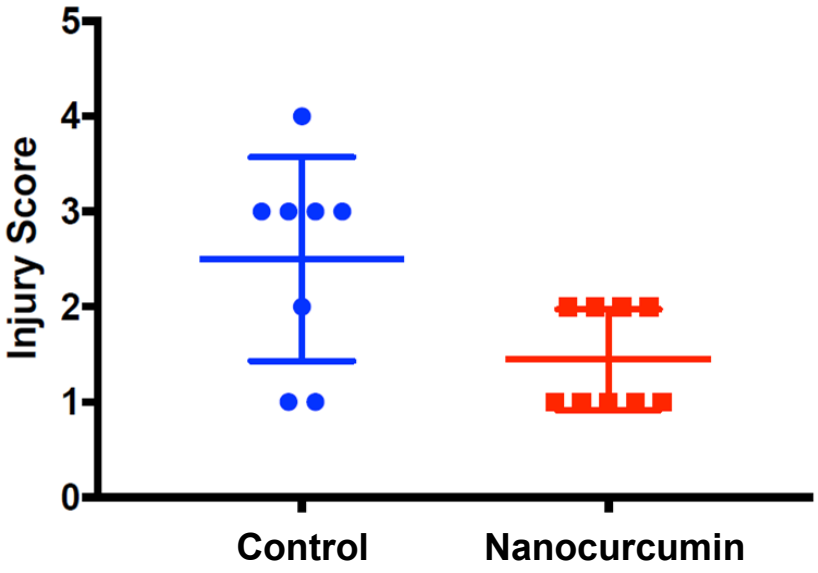

4.3 Discussion

In this chapter, the single emulsion method with 1% (w/v) PVA and EtAc were used to formulate curcumin-loaded mPEG5k-PLGA45k (50:50) nanoparticles. P7 Sprague Dawley HI rats were used. Area loss assessment and injury severity score were used to evaluate the neuroprotective efficacy of the curcumin-loaded nanoparticles. Area loss assessment showed no significant neuroprotection with the curcumin-loaded nanoparticles, while injury severity score did show the rats treated with curcumin-loaded nanoparticles had a lower average injury score compared with rats treated with saline.

There are a couple of potential reasons for the difference between these two assessments. The area loss score was a rough estimate of only one brain slice from each brain. Triphenyl tetrazolium chloride (TTC) staining was evaluated at a single level; however, researchers typically use haematoxylin and eosin (H&E) stained slides at multiple levels and average across all levels. This provides an area loss across a greater area of the brain. Moreover, the area loss assessment by TTC was completed seven days after the HI injury. Since TTC staining accuracy is not as high 72 h after HI injury, the TTC analysis technique 7 days after HI could be inaccurate. Future studies should evaluate TTC at P10, 3 days after injury, and across the entire brain.

Furthermore, the injury severity score is subjective and is semi-quantitative. Factors such as the angle of the photo and researcher to researcher differences in evaluating could alter the scoring. However, the injury severity score assesses the whole hemisphere, while the area loss assessment does not. As a result, if the part of the brain we looked at for the area loss assessment was not

improved by curcumin, but we saw some benefits for the hemisphere as a whole, then a difference between the results from these two measurements would occur. Moreover, only eight rats were used in each group (typically 20 rats per group are required), and the curcumin-loaded nanoparticle was not the optimized nanoparticle. Accordingly, these were two additional factors that would affect the ability to evaluate curcumin's efficacy in these preliminary studies.

Overall, in this chapter, two groups consisting of eight HI rats per group were preliminarily used to evaluate curcumin-loaded nanoparticle's therapeutic effect on providing better neuroprotection and reduced neuronal injury in the neonatal HI rats. Preliminarily, curcumin-loaded nanoparticle made from the single emulsion method with 1% (w/v) PVA and EtAc did give a trend towards neuroprotection and help reduce neuronal injury in the neonatal HI rats. However, as described previously, there were still some potential factors influencing the result. In the future, increasing animal numbers per group with the optimized nanoparticle formulation and appropriate efficacy assessments will be done. Furthermore, except for area loss assessment and injury severity score, histopathology, neuropathology and some behavior studies will also be included to evaluate curcumin-loaded nanoparticle's therapeutic effect. These would provide a more holistic understanding of the therapeutic capability of a curcumin-loaded nanoparticle.

4.4 Conclusion

In chapter 2 and 3, we were able to successfully formulate stable curcumin-loaded mPEG5k-PLGA45k (50:50) nanoparticle with sub-60 nm in size, nearly neutral ζ-potential, fine curcumin loading and a sustained curcumin release over 24 to 48 h. We also demonstrated mPEG5k-

PLGA45k (50:50) nanoparticles were able to diffuse within the brain parenchyma, cross the impaired BBB and deliver curcumin into the brain. In this chapter, we provide preliminary data that demonstrated curcumin-loaded nanoparticles made from the single emulsion method with 1% (w/v) PVA and EtAc did give a trend towards neuroprotection and help reduce neuronal injury in the neonatal HI rats. We are currently repeating this efficacy study with our optimized nanoparticle platform, and including a blank nanoparticle group, with twenty P7 rats per group. We are still working on analyzing the results to demonstrate curcumin-loaded nanoparticle's efficacy on providing neuroprotection and reducing neuronal injury in the neonatal P7 HI rats.

References

1. Fatemi, A., M.A. Wilson, and M.V. Johnston, *Hypoxic-ischemic encephalopathy in the term infant.* Clin Perinatol, 2009. **36**(4): p. 835-58, vii.
2. Lai, M.C. and S.N. Yang, *Perinatal hypoxic-ischemic encephalopathy.* J Biomed Biotechnol, 2011. **2011**: p. 609813.
3. Jacobs, S.E., et al., *Cooling for newborns with hypoxic ischaemic encephalopathy.* Cochrane Database Syst Rev, 2013(1): p. CD003311.
4. Shankaran, S., *Therapeutic hypothermia for neonatal encephalopathy.* Curr Treat Options Neurol, 2012. **14**(6): p. 608-19.
5. Silveira, R.C. and R.S. Procianoy, *Hypothermia therapy for newborns with hypoxic ischemic encephalopathy.* J Pediatr (Rio J), 2015. **91**(6 Suppl 1): p. S78-83.
6. Sameshima, H. and T. Ikenoue, *Hypoxic-ischemic neonatal encephalopathy: animal experiments for neuroprotective therapies.* Stroke Res Treat, 2013. **2013**: p. 659374.
7. Yuan, J. and B.A. Yankner, *Apoptosis in the nervous system.* Nature, 2000. **407**(6805): p. 802-9.
8. Northington, F.J., E.M. Graham, and L.J. Martin, *Apoptosis in perinatal hypoxic-ischemic brain injury: how important is it and should it be inhibited?* Brain Res Brain Res Rev, 2005. **50**(2): p. 244-57.
9. Wassink, G., et al., *The mechanisms and treatment of asphyxial encephalopathy.* Front Neurosci, 2014. **8**: p. 40.
10. Drury, P.P., L. Bennet, and A.J. Gunn, *Mechanisms of hypothermic neuroprotection.* Semin Fetal Neonatal Med, 2010. **15**(5): p. 287-92.
11. Gluckman, P.D., et al., *Selective head cooling with mild systemic hypothermia after neonatal encephalopathy: multicentre randomised trial.* Lancet, 2005. **365**(9460): p. 663-70.
12. Azzopardi, D.V., et al., *Moderate hypothermia to treat perinatal asphyxial encephalopathy.* N Engl J Med, 2009. **361**(14): p. 1349-58.
13. Shankaran, S., et al., *Whole-body hypothermia for neonates with hypoxic-ischemic encephalopathy.* N Engl J Med, 2005. **353**(15): p. 1574-84.
14. Eicher, D.J., et al., *Moderate hypothermia in neonatal encephalopathy: efficacy outcomes.* Pediatr Neurol, 2005. **32**(1): p. 11-7.
15. Lin, Z.L., et al., *Mild hypothermia via selective head cooling as neuroprotective therapy in term neonates with perinatal asphyxia: an experience from a single neonatal intensive care unit.* J Perinatol, 2006. **26**(3): p. 180-4.
16. Tagin, M.A., et al., *Hypothermia for neonatal hypoxic ischemic encephalopathy: an updated systematic review and meta-analysis.* Arch Pediatr Adolesc Med, 2012. **166**(6): p. 558-66.
17. Massaro, A.N., et al., *Neonatal neurobehavior after therapeutic hypothermia for hypoxic ischemic encephalopathy.* Early Hum Dev, 2015. **91**(10): p. 593-9.
18. Fleiss, B., et al., *Inflammation-induced sensitization of the brain in term infants.* Dev Med Child Neurol, 2015. **57 Suppl 3**: p. 17-28.

19. Smit, E., et al., *Cooling neonates who do not fulfil the standard cooling criteria - short- and long-term outcomes.* Acta Paediatr, 2015. **104**(2): p. 138-45.
20. McPherson, R.J. and S.E. Juul, *Erythropoietin for infants with hypoxic-ischemic encephalopathy.* Curr Opin Pediatr, 2010. **22**(2): p. 139-45.
21. Park, D., et al., *Protective effects of N-acetyl-L-cysteine in human oligodendrocyte progenitor cells and restoration of motor function in neonatal rats with hypoxic-ischemic encephalopathy.* Evid Based Complement Alternat Med, 2015. **2015**: p. 764251.
22. Sabir, H., et al., *Xenon Combined with Therapeutic Hypothermia Is Not Neuroprotective after Severe Hypoxia-Ischemia in Neonatal Rats.* PLoS One, 2016. **11**(6): p. e0156759.
23. Yager, J.Y., E.A. Armstrong, and A.M. Black, *Treatment of the term newborn with brain injury: simplicity as the mother of invention.* Pediatr Neurol, 2009. **40**(3): p. 237-43.
24. Gupta, S.K., et al., *Curcumin prevents experimental diabetic retinopathy in rats through its hypoglycemic, antioxidant, and anti-inflammatory mechanisms.* J Ocul Pharmacol Ther, 2011. **27**(2): p. 123-30.
25. Wu, A., et al., *Curcumin boosts DHA in the brain: Implications for the prevention of anxiety disorders.* Biochim Biophys Acta, 2015. **1852**(5): p. 951-61.
26. Esatbeyoglu, T., et al., *Curcumin--from molecule to biological function.* Angew Chem Int Ed Engl, 2012. **51**(22): p. 5308-32.
27. Liao, K.K., et al., *Curcuminoids promote neurite outgrowth in PC12 cells through MAPK/ERK- and PKC-dependent pathways.* J Agric Food Chem, 2012. **60**(1): p. 433-43.
28. Kim, S.J., et al., *Curcumin stimulates proliferation of embryonic neural progenitor cells and neurogenesis in the adult hippocampus.* J Biol Chem, 2008. **283**(21): p. 14497-505.
29. Kang, S.K., et al., *Autologous adipose tissue-derived stromal cells for treatment of spinal cord injury.* Stem Cells Dev, 2006. **15**(4): p. 583-94.
30. Kulkarni, S.K. and A. Dhir, *An overview of curcumin in neurological disorders.* Indian J Pharm Sci, 2010. **72**(2): p. 149-54.
31. Prasad, S., A.K. Tyagi, and B.B. Aggarwal, *Recent developments in delivery, bioavailability, absorption and metabolism of curcumin: the golden pigment from golden spice.* Cancer Res Treat, 2014. **46**(1): p. 2-18.
32. Anand, P., et al., *Bioavailability of curcumin: problems and promises.* Mol Pharm, 2007. **4**(6): p. 807-18.
33. Curtis, C., et al., *Systems-level thinking for nanoparticle-mediated therapeutic delivery to neurological diseases.* Wiley Interdiscip Rev Nanomed Nanobiotechnol, 2017. **9**(2).
34. Alavijeh, M.S., et al., *Drug metabolism and pharmacokinetics, the blood-brain barrier, and central nervous system drug discovery.* NeuroRx, 2005. **2**(4): p. 554-71.
35. Davis, M.E., Z.G. Chen, and D.M. Shin, *Nanoparticle therapeutics: an emerging treatment modality for cancer.* Nat Rev Drug Discov, 2008. **7**(9): p. 771-82.
36. Petros, R.A. and J.M. DeSimone, *Strategies in the design of nanoparticles for therapeutic applications.* Nat Rev Drug Discov, 2010. **9**(8): p. 615-27.
37. Peer, D., et al., *Nanocarriers as an emerging platform for cancer therapy.* Nature Nanotechnology, 2007. **2**(12): p. 751-760.
38. Nance, E.A., et al., *A dense poly(ethylene glycol) coating improves penetration of large polymeric nanoparticles within brain tissue.* Sci Transl Med, 2012. **4**(149): p. 149ra119.
39. Makadia, H.K. and S.J. Siegel, *Poly Lactic-co-Glycolic Acid (PLGA) as Biodegradable Controlled Drug Delivery Carrier.* Polymers (Basel), 2011. **3**(3): p. 1377-1397.

40. Gref, R., et al., *Biodegradable long-circulating polymeric nanospheres.* Science, 1994. **263**(5153): p. 1600-3.
41. Kulkarni, S.A. and S.S. Feng, *Effects of surface modification on delivery efficiency of biodegradable nanoparticles across the blood-brain barrier.* Nanomedicine (Lond), 2011. **6**(2): p. 377-94.
42. Xu, Q., et al., *Scalable method to produce biodegradable nanoparticles that rapidly penetrate human mucus.* J Control Release, 2013. **170**(2): p. 279-86.
43. Tabatabaei Mirakabad, F.S., et al., *A Comparison between the cytotoxic effects of pure curcumin and curcumin-loaded PLGA-PEG nanoparticles on the MCF-7 human breast cancer cell line.* Artif Cells Nanomed Biotechnol, 2016. **44**(1): p. 423-30.
44. Yang, M., et al., *Nanoparticle penetration of human cervicovaginal mucus: the effect of polyvinyl alcohol.* J Control Release, 2014. **192**: p. 202-8.
45. McCall, R.L. and R.W. Sirianni, *PLGA nanoparticles formed by single- or double-emulsion with vitamin E-TPGS.* J Vis Exp, 2013(82): p. 51015.
46. Yoo, H.S., et al., *Biodegradable nanoparticles containing doxorubicin-PLGA conjugate for sustained release.* Pharm Res, 1999. **16**(7): p. 1114-8.
47. Valentine, M.T., et al., *Colloid surface chemistry critically affects multiple particle tracking measurements of biomaterials.* Biophys J, 2004. **86**(6): p. 4004-14.
48. Suh, J., M. Dawson, and J. Hanes, *Real-time multiple-particle tracking: applications to drug and gene delivery.* Adv Drug Deliv Rev, 2005. **57**(1): p. 63-78.
49. Wood, T., et al., *Treatment temperature and insult severity influence the neuroprotective effects of therapeutic hypothermia.* Sci Rep, 2016. **6**: p. 23430.
50. Wu, Y.W., et al., *High-Dose Erythropoietin and Hypothermia for Hypoxic-Ischemic Encephalopathy: A Phase II Trial.* Pediatrics, 2016. **137**(6).
51. Smit, E., et al., *The effect of resuscitation in 100% oxygen on brain injury in a newborn rat model of severe hypoxic-ischaemic encephalopathy.* Resuscitation, 2015. **96**: p. 214-9.
52. Baker, S.P. and B. O'Neill, *The injury severity score: an update.* J Trauma, 1976. **16**(11): p. 882-5.